# Phylogenetic signatures of ecological divergence and leapfrog adaptive radiation in Espeletia

Charles Pouchon, Sébastien Lavergne, Ángel Fernández, Adriana Alberti, Serge Aubert, Jesus Mavarez

RESEARCH ARTICLE

Short Title: Pouchon et al.— Adaptive radiation in *Espeletia*

# Phylogenetic signatures of ecological divergence and leapfrog adaptive radiation in *Espeletia*

Charles Pouchon[1], Sébastien Lavergne[1], Ángel Fernández[2], Adriana Alberti[3], Serge Aubert[1,4,†], and Jesús Mavárez[1,5]

Manuscript received 16 April 2020; revision accepted 21 September 2020

[1] Laboratoire d'Ecologie Alpine (LECA), Univ. Grenoble Alpes, Univ. Savoie Mont Blanc, CNRS, F-38000 Grenoble, France

[2] Herbario IVIC. Instituto Venezolano de Investigaciones Científicas, Apartado 20632, Caracas 1020-A, Venezuela.

[3] Génomique Métabolique, Genoscope, Institut François Jacob, CEA, CNRS, Université Evry, Université Paris-Saclay, 91057 Evry, France.

[4] Université Grenoble Alpes, CNRS, Université Savoie Mont Blanc, SAJF, Station Alpine Joseph Fourier, 38000 Grenoble, France.

[5] Author for correspondence (e-mail: jesus.mavarez@univ-grenoble-alpes.fr); ORCID id: 0000-0002-2483-0178

[†] Serge Aubert: 1966–2015.

**Citation:** Pouchon, C., S. Lavergne, Á. Fernández, A. Alberti, S. Aubert, and J. Mavárez. 2021. Phylogenetic signatures of ecological divergence and leapfrog adaptive radiation in *Espeletia*. *American Journal of Botany* 108(1): XXXX.

**DOI: XXXX**

**PREMISE**: Events of accelerated species diversification represent one of Earth's most celebrated evolutionary outcomes. Northern Andean high-elevation ecosystems, or páramos, host some plant lineages that have experienced the fastest diversification rates, likely triggered by ecological opportunities created by mountain uplifts, local climate shifts, and key trait innovations. However, the mechanisms behind rapid speciation into the new adaptive zone provided by these opportunities have long remained unclear.

**METHODS**: We address this issue by studying the Venezuelan clade of *Espeletia*, a species-rich group of páramo-endemics showing a dazzling ecological and morphological diversity. We performed several comparative analyses to study both lineage and trait diversification, using an updated molecular phylogeny of this plant group.

**RESULTS**: We showed that sets of either vegetative or reproductive traits have conjointly diversified in *Espeletia* along different vegetation belts, leading to adaptive syndromes. Diversification in vegetative traits occurred earlier than in reproductive ones. The rate of species and morphological diversification showed a tendency to slow down over time, probably due to diversity dependence. We also found that closely related species exhibit significantly more overlap in their geographic distributions than distantly related taxa, suggesting that most events of ecological divergence occurred at close geographic proximity within páramos.

**CONCLUSIONS**: These results provide compelling support for a scenario of small-scale ecological divergence along multiple ecological niche dimensions, possibly driven by competitive interactions between species, and acting sequentially over time in a leapfrog pattern.

**KEY WORDS:** Andes, Asteraceae, caulescent rosettes, evolution, frailejón, high-elevation ecosystems, páramo, speciation, species diversification.

Evolutionary radiations, defined as events of accelerated species diversification on relatively short timescales (Simões et al., 2016), have often been documented in many high mountain floras, such as the Rockies (Drummond, 2008), the New Zealand Alps (Joly et al., 2014), the Himalayas and Hengduan Mountains (Ebersbach et al., 2017), New Guinea (Brown et al., 2006), the European Alps (Roquet et al., 2013), and the tropical Andes (Madriñán et al., 2013). The ecological and historical setting of these high-elevation plant radiations likely implies some sort of ecological opportunities provided by mountain uplifts and climatic shifts (Hughes and Atchison, 2015), and by the evolution of key trait innovations allowing the colonization of new adaptive zones (sensu Simpson, 1944). Some of the best examples of key innovations for high-elevation habitats in plants are specialized growth-forms such as cushions (Boucher et al., 2016a) and caulescent rosettes (Monasterio and Sarmiento, 1991; Pouchon et al., 2018), as well as stem woodiness (Nürk et al., 2019) and several freezing-avoidance mechanisms (Rada, 2016), which clearly improved adaptation to life in these relatively cold, dry, and irradiated environments. However, the precise mechanisms of increased speciation rate within this adaptive zone remain uncertain. For instance, under a scenario of ecological opportunity, speciation could be triggered either by neutral processes such as the relative isolation and fragmentation of high-elevation habitats favoring allopatric speciation without niche differentiation (Boucher et al., 2016b), or alternatively, by disruptive selection favoring ecological speciation (Lagomarsino et al., 2016), as expected in adaptive radiations (Schluter, 2000).

Comparative methods involving phylogenies and trait data are particularly useful to study the outcome of ecological and neutral processes acting on species radiations through different evolutionary models (Glor, 2010; Pyron and Burbrink, 2013; Soulebeau et al., 2015). Under a scenario of predominant adaptive divergence, sympatric lineages should specialize ecologically on distinct resources, leading to reduced competition and ecological speciation (Schluter, 2000; Givnish, 2015). Consequently, when lineages undergo adaptive radiations in a bounded ecological space, species' phylogenies should bear signatures of diversity-dependence on diversification rates of both lineages and traits (Rabosky, 2009; Nuismer and Harmon, 2015). This could be highlighted by a slowdown in diversification rate towards the present, as species accumulate within a delimited adaptive zone (e.g., the 'time-dependent' and 'diversity-dependent' models; Gavrilets and Losos, 2009; Harmon et al., 2010) or by competition models in which trait divergence depends on the available phenotypic space (e.g., 'Matching competition' models; Drury et al., 2016; Aristide and Morlon, 2019). Adaptive phenotypic divergence should therefore be particularly evident between recently diverged species occurring in sympatry. However, despite a wealth of phylogenetic studies of evolutionary radiations in

mountain environments (Weir, 2006; Drummond et al., 2012; Madriñán et al., 2013; Price et al., 2014), these expected patterns have remained relatively elusive among high-elevation biomes (Nevado et al., 2019), probably because of a blurring of the adaptive signal by non-adaptive divergence (Rundell and Price, 2009) and/or lack of appropriate phylogenetic resolution (Glor, 2010).

High-elevation environments are notoriously heterogeneous in soil conditions, topography, and exposition, thus allowing many niche dimensions – that is, many axes of ecological divergence for natural selection to act upon. It is unclear to what extent the increased diversification rates observed in these environments are driven by biotic or abiotic factors, or a combination of both. Recent phylogenetic studies of Andean plant clades have showed that speciation has been mainly triggered by divergence in relation to biotic factors such as pollinators and dispersal agents (Lagomarsino et al., 2016, 2017), or to abiotic factors distributed along environmental gradients (Testo et al., 2019). Moreover, these drivers of speciation may not only vary in space but also more importantly in time, which could make the phylogenetic signatures of ecological divergence difficult to detect. Indeed, Grant (1949) hypothesized that diversification for reproductive traits should occur prior to diversification for vegetative traits in lineages depending on specialized pollinators. With similar reasoning, Chase and Palmer (1997) proposed that plant clades could undergo adaptive radiation in a 'leapfrog' fashion, by adapting first to novel habitat opportunities, and then to novel biotic factors. A recent study on New Caledonian *Oxera* Labill. [Lamiaceae] tested these hypotheses and showed that this clade diversified due to varied ecological and biological drivers, perhaps acting in a leapfrog pattern, but that geographic processes played an equally important role (Barrabé et al., 2019). This has encouraged us to wonder about the prevalence of leapfrog patterns and ecological divergences in contrast to neutral processes during the temporal building of high-elevation radiations, particularly in the Andes.

Páramos, which are high-elevation ecosystems located between the upper tree-line (ca. 3200 m a.s.l.) and glacier limits (ca. 4800 m a.s.l.) in the Andes of Venezuela, Colombia, Ecuador, and northern Peru, provide an ideal setting to study the evolutionary processes that drove plant radiations. Indeed, páramos occupy a relatively small area (ca. 35,000 $km^2$; Josse et al., 2009), have a recent origin (ca. 2.7 Ma; Gregory-Wodzicki, 2000; Hooghiemstra et al., 2006; Torres et al., 2013) and are characterized by relatively harsh conditions (e.g., low average temperatures, extreme day-night temperature oscillations; Luteyn, 1999). Four vegetation belts are usually considered for páramos according to climate and vegetation structure (Van der Hammen and Cleef, 1986): the upper part of the Andean forest (ca. 2500–

3200 masl); the transitory shrubby sub-páramo (ca. 3200–3500 m a.s.l.); the open grass páramo (hereafter "proper páramo") (ca. 3500–4200 m a.s.l.); and the rocky and sandy super-páramo (ca. 4200 masl to the lower limit of glaciers). Yet, páramos are extraordinarily species-rich and are host to some of the fastest plant radiations on Earth (Madriñán et al., 2013), probably owing to their high environmental heterogeneity and their dynamic history of habitat connectivity during the Pleistocene (Antonelli and Sanmartín, 2011; Flantua et al., 2019). Many cases of rapid species diversification have thus been documented in páramos, such as in the genera *Lupinus* L. [Fabaceae] (Nevado et al., 2016, 2018), *Bartsia* L. [Orobanchaceae] (Uribe-Convers and Tank, 2015), *Hypericum* L. [Hypericaceae] (Nürk et al., 2013), *Diplostephium* Kuntz [Asteraceae] (Vargas et al., 2017) and *Espeletia* Mutis ex Bonpl. (Diazgranados and Barber, 2017; Pouchon et al., 2018).

The genus *Espeletia* (Asteraceae, Millerieae) presently comprises about 140 species endemic to the páramos of Venezuela, Colombia, and northern Ecuador (see Fig. 1A). It evolved from a single ancestor in less than 2.5 Ma, i.e., after the final uplift of the northern Andes, and has two reciprocally monophyletic groups: (1) a group including species distributed exclusively in the Colombian Andes plus one species reaching northern Ecuador (hereafter Colombian clade); and (2) a group mostly composed by species distributed exclusively in the Venezuelan Cordillera de Mérida plus a few taxa from northeastern Colombia (hereafter Venezuelan clade) (Diazgranados and Barber, 2017; Pouchon et al., 2018). The genus exhibits important morphological diversity for vegetative and reproductive traits, particularly regarding growth forms (i.e., trees, shrubs, caulescent rosettes), reproductive systems (i.e., monocarpic and polycarpic species), and pollination vectors (i.e., wind or insects) (Smith, 1981; Berry and Calvo, 1989; Diazgranados, 2012; Cuatrecasas, 2013; Mavárez, 2019) (Fig. 1C). Many species in *Espeletia*, particularly among caulescent rosettes, exhibit a series of morphological and physiological traits with presumably high adaptive value in the relatively harsh environments of páramos, such as covering of stems by the remains of dead leaves, large pith volumes, dense leaf pubescence, and super-cooling capacity (Luteyn, 1999; Rada, 2016). In addition, *Espeletia* shows large ecological variation for habitat preferences, i.e., from wetlands to open landscapes and dry rocky slopes, and from the upper limit of the Andean forests to the edge of glaciers in super-páramo habitats (ca. 2500-4800 m a.s.l.) (Fig. 1B).

All this wealth of morphological and ecological diversity in *Espeletia* developed after the evolution of the caulescent rosette growth-form in the common ancestor of the genus, which may have provided the initial key innovation allowing the occupation of the newly created adaptive zone of

páramos (Cuatrecasas, 2013; Pouchon et al., 2018). However, as for most high-elevation plant lineages, the main drivers of such diversity in *Espeletia* remain uncertain. Allopatry appears to be predominant in the Colombian clade of *Espeletia* across páramos while ecological speciation seems to have occurred at a microenvironment level (Padilla-González et al., 2017; Cortés et al., 2018). Hence, we can legitimately wonder how ecological and geographical processes have driven speciation in the Venezuelan clade of *Espeletia*, which exhibits a larger degree of morphological and ecological variation than its Colombian counterpart (Cuatrecasas, 2013; Pouchon et al., 2018; Mavárez, 2019). We posit that arrays of vegetative traits related to habitat preference (e.g., growth-form, ramification capacity, stem height, etc.) or reproductive traits linked to pollination strategy (e.g., inflorescence size, capitulum diameter, flower orientation, etc.) have probably co-evolved along environmental gradients, forming different adaptive trait syndromes during the diversification of *Espeletia*. Furthermore, since the spatiotemporal set-up behind the possible evolution of these vegetative and reproductive trait syndromes would not necessarily be the same, we can legitimately wonder whether they diverged following different dynamics, i.e., in a leapfrog pattern.

Here we performed a detailed comparative analysis of trait evolution and species diversification within the Venezuelan clade of *Espeletia*. Our goal was to untangle the ecological and neutral drivers of diversification in this plant group by benefiting from the genomic approach developed by Pouchon et al. (2018) to resolve its phylogenetic relationships. We tested for phylogenetic predictions derived from scenarios of ecological divergence, such as whether: (1) sympatry is more prevalent between closely related species; (2) sets of vegetative or reproductive traits conjointly diverge between species occupying different habitats, leading to different adaptive syndromes; (3) vegetative and reproductive trait syndromes diverge possibly at different time-periods in a leapfrog pattern; and (4) rates of phenotypic diversification for these traits combinations show diversity-dependence. We also tested whether rates of species diversification change through time in relation to the species diversity (i.e., biotic factors), or as a function of variations in paleo-temperatures during Pleistocene climatic changes (i.e., abiotic factors).

## <h1>MATERIALS AND METHODS

### <h2>Sampling, DNA extraction, and shotgun sequencing

We aimed to complete the sampling of species in the Venezuelan clade of *Espeletia* in comparison to our previous phylogenetic analysis (Pouchon et al., 2018). To achieve this, we sampled one individual

from 18 additional *Espeletia* species, 16 belonging to the Venezuelan clade and two in the Colombian clade, plus the additional outgroup taxon *Ichthyothere garciabarrigae* H.Rob. [Asteraceae] (Appendix S1). To evaluate the efficiency of our approach at resolving phylogenetic relationships between and within species we also sampled additional individuals for some species. In each case, leaf samples were collected, most of their pubescence removed with razor blades directly in the field and dried with silica gel in airtight plastic bags. Genomic DNA was extracted from dried leaf fragments according to the protocol described in Pouchon et al. (2018). Shotgun libraries were prepared and sequenced (2 × 150 bp paired-ends) in an Illumina HiSeq 4000 at the French National Sequencing Center (Genoscope, Évry, France) or in an Illumina Hiseq 2000 at Fasteris (Geneva, Switzerland) (Appendix S1). In total, combined with the sequence reads of 34 species in the Venezuelan clade of *Espeletia* retrieved from Pouchon et al. (2018), we generated a new dataset of 50 species representing 92.5% of the 54 recognized in this clade (Mavárez, 2019), seven species in the Colombian clade, and three external outgroups.

**<h2>Alignments, phylogenetic inference, and dating**

Sequence reads (ca. 13 million reads per sample, Appendix S2b), were filtered based on a Phred score quality value of 20 using the FASTX toolkit (http://hannonlab.cshl.edu/fastx_toolkit/). In a recent study, Pouchon et al. (2018) first produced a set of 9880 nuclear multi-species' metacontigs loci from the assembly of single-species' contigs, which served afterwards as a reference to align the reads of each species that were used for the phylogenetic analyses in *Espeletia* (Appendix S2a). Here, we applied this procedure from its second step, by mapping directly the filtered reads into all the 9880 metacontigs of Pouchon et al. (2018) using BWA version 0.7.5 (Li and Durbin, 2009) (Appendix S2a). In order to reduce paralogs for each taxon we kept only reads mapping to a single metacontigs with a minimum MAPQ score of 60 for the variant calling, by using the 'mpileup' workflow of SAMtools version 0.1.19 and BCFtools version 0.1.19 (Li et al., 2009). Finally, a consensus sequence alignment was generated by metacontig from the variant call format file using the vcfutils script (supplied with SAMtools), and by filtering variants with a root-mean-square of the mapping quality ≥ 15 and a minimum read coverage of 10 per taxon.

Phylogenetic reconstructions were made from the concatenation of all consensus alignments, resulting in a median of 6629 alignments per sample (Appendix S2b), by using Maximum Likelihood (ML) in RAxML-HPC version 8.2.9 (Stamatakis, 2006) and Bayesian inference in ExaBayes version 1.4.1 (Aberer et al., 2014). The ML analysis was performed using a GTRGAMMAI substitution model

and 500 bootstrap replicates. Bayesian inference was conducted using the default values for temperatures of chain heating and the number of Metropolis-coupled Markov chain Monte Carlo (MCMC) under 500,000 generations. We assessed chain convergence and mixing using summary statistics of the postProcParam function in ExaBayes (Aberer et al., 2014). We used a minimum sample size of 200 to estimate each model parameter, and kept the similarity within and between chain-variance with a potential scale reduction factor below and close to 1. A 50% majority-rule consensus phylogram with posterior probabilities was obtained using the ExaBayes consense function with a burnin fraction of 25%.

Calibration of divergence times was performed according to the approach followed for the nuclear dataset described in Pouchon et al. (2018), using the 2.0–2.6 Ma estimate of the age for the crown node of *Espeletia* as a constraint for estimating divergence times in r8s version 1.7.1 (Sanderson, 2003). Uncertainty in the estimation of divergence time was assessed using 200 Bayesian trees randomly selected from the stationary distribution of the MCMC. Cross-validation was conducted on each tree replicate to determine the optimal level of smoothing-rate for 100 estimates starting with a log10 value of -5 and increments of 0.4. Finally, mean values and 95% confidence intervals for each node age were estimated from the chronograms using TreeAnnotator (Drummond et al., 2012a). We randomly selected 100 dating trees, pruned to the species level, to incorporate topological uncertainty in the diversification analyses.

**<h2>Geographic range overlap**

We estimated the geographic range overlap between all species' pairs to describe the geographic context of recent speciation processes. Based on the distribution of species on the main geographic units of páramos (adapted from Mavárez, 2019; see Fig. 3B, Appendix S3), we estimated the degree of sympatry across all páramo units for all species' pairs in the phylogeny, using the Pianka index as implemented in the R package 'spaa' version 0.2.2 (Zhang, 2016). This index quantifies the frequency at which two species co-occur in the geographic units, with a value ranging from 0 (no co-occurrence) to 1 (co-occurrence in all units). We tested for the correlation between the range overlap of species' pairs and their phylogenetic distance, using a mantel correlogram as implemented in the R package 'vegan' version 2.5.4 (Oksanen et al., 2018). A comparison in range overlap was also made between sister and non-sister species to document how geographic ranges of species diverged right after speciation events.

## <h2>Models of lineage diversification

We tested whether past rates of species diversification varied with time, climate, or species-diversity. The sampling fraction of taxa was set to 0.925 (50/54) for each model. Models were compared using the corrected Akaike Information Criterion (AICc), with ΔAICc > 2 to pick the best model following the advice of Burnham and Anderson (2002). Moreover, as extinction rates are hardly estimable with current statistical approaches applied on molecular phylogenies (Rabosky, 2010), only models allowing variations in speciation rate were fitted to avoid the potential flaws recently highlighted by Burin et al. (2019) on models assuming temporally variable extinction rates.

### *<h3>Time dependent models*

We compared models assuming that clade growth follows Pure Birth (PB) or Birth-Death (BD) processes, as well as BD models with speciation rate that change through time in exponential (BDX+T) fashion under a constant extinction rate. These analyses were performed in R using the package 'RPANDA' version 1.5 (Morlon et al., 2016). Linear-dependent models as implemented in 'RPANDA' were not used in this analysis given the recent concern raised by their possible estimation of negative speciation rates (Gamisch, 2020). Variation of speciation rate through time was also explored in a Bayesian analysis using BAMM version 2.5.0, also assuming a constant extinction rate as above (Rabosky, 2014) (Appendix S4).

### *<h3>Climate dependent models*

Global paleo-temperatures were retrieved from Zachos et al. (2008) and used to test for their direct exponential relation with the speciation rates (BDX+E). These models were fitted in 'RPANDA', following the approach of Morlon et al. (2011). As above, linear-dependent models were not considered in this analysis (Gamisch, 2020).

### *<h3>Diversity dependent models*

We fitted models in which speciation rate follows linear or exponential dependence with species diversity under constant extinction rate (DDL and DDX models). We compared them to PB and BD models using the R package 'DDD' version 4.0 (Etienne et al., 2012). Each model inference was initiated with a clade-level carrying capacity K = 54 (which equals contemporary species diversity in the Venezuelan clade of *Espeletia*).

## <h2>Characterization of species' morphologies, climatic niches, and habitats

### *<h3>Morphology*

In order to estimate how different sets of traits have co-evolved to form vegetative or reproductive trait syndromes, we selected a total of five vegetative and six reproductive characters, including both quantitative and discrete, depicting the morphological diversity of study species (Mavárez, 2019), given in Table 1. Quantitative traits were scaled, and a Principal Component Analysis of mixed data (PCAmix) was performed with the R package 'ade4' version 1.7.13 (Dray and Dufour, 2007) separately for vegetative and reproductive traits to reduce trait dimensionality and therefore identify trait syndromes using both quantitative and discrete traits. We used the position of each species along the different axes as new composite morphological trait (i.e., trait combinations) for further analyses.

### *<h3>Niches*

To estimate the climatic niche of species, 1755 geo-referenced occurrence points were collected for the study species from Mavárez (2019) (i.e., a median of 26 points/species). To reduce pseudo-replication between sampling localities, we kept for each species only one occurrence per 30 arc-second grid cell (ca. 900 m × 900 m resolution). For each record, we extracted values for elevation, aspect, and slope from a digital elevation model, together with values for the 19 climatic variables of the WorldClim dataset (Fick and Hijmans, 2017). Niche positions were estimated using the Outlying Mean Index (OMI; Dolédec et al., 2000) following the procedure of Thuiller et al. (2004).

### *<h3>Habitats*

We used the habitat preferences of each species into the four vegetation belts of páramos (i.e., upper Andean forest, sub-páramo, proper páramo, super-páramo). Distribution of species in these habitats was retrieved from Cuatrecasas (2013) and Mavárez (2019). A Multiple Correspondence Analysis (MCA) was performed to capture the position of each species into these vegetation belts, using 'ade4' (Dray and Dufour, 2007).

## <h2>Trait-environment correlations

The ensemble of data depicting species' positions on axes for morphological variation, environmental gradients and habitat preferences were analyzed against each other using phylogenetic generalized least squares (PGLS) regressions with R packages 'caper' version 1.0.1 (Orme et al., 2018) and 'ape'

version 5.4-1 (Paradis et al., 2020). This helped to identify which combinations of traits show consistent relationships with particular niches or habitats, while accounting for species' phylogenetic relatedness. Phylogenetic relationships used in the PGLS were derived from the time-calibrated tree. We tested all possible relationships between each type of morphologic variation (PCAmix axes) and niches (OMI axes) or habitats (MCA axes) using likelihood ratio tests. As we performed multiple tests, a correction was used on *p*-values (Benjamini and Hochberg, 1995). We also conducted these analyses separately on the quantitative traits composing these PCA axes to investigate whether particular traits follow the same evolutionary trajectories as the morphological syndromes they belong to.

**<h2>Models of trait evolution**

To understand how the sets of vegetative and reproductive traits have co-evolved during the radiation, we fitted seven phylogenetic models of trait evolution to the vegetative and reproductive PCAmix axes described above: (1) the Brownian Motion model (BM), assuming a random walk of trait evolution; (2) the Ornstein-Uhlenbeck model (OU), assuming constrained trait evolution toward a single optimum; (3) the Early-Burst model (EB), assuming an exponential decrease of evolutionary rates over time, concordant with a "niche filling" scenario (Harmon et al., 2010); (4) the Delta model, analogous to the EB model, assuming a time-dependent trait evolution by contrasting early and late evolution; (5) the Matching Competition model (MC), assuming variation of trait in a lineage as a function of trait values in other lineages; and (6-7) two Diversity-Dependent models, assuming that trait evolutionary rates vary as a linear (DDL) or exponential (DDX) function of the number of lineages. Models BM, OU, Delta and EB were fitted in the R package 'geiger' version 2.0.6.1 (Harmon et al., 2008) whereas models MC, DDL, and DDX were fitted in 'RPANDA' (Morlon et al., 2016), as in Drury et al. (2016). Goodness-of-fit was determined using AICc. We compared the tempo of trait diversification between vegetative and reproductive trait combinations from the estimates of the Pagel's delta parameter ($\delta$) of the Delta model on each PCAmix axis separately. This parameter depicts whether a given trait mostly diversified early in time with a slowdown to the present (i.e., in deep branches, $\delta < 1$) or rather later in time (i.e., in recent branches, $\delta > 1$).

We also visualized the evolutionary trajectories of both types of traits through time using the phenogram function implemented in the 'phytools' version 0.6.60 R package (Revell, 2012) with uncertainty at ancestral nodes and along branches. This allowed testing whether a sequential divergence in vegetative and reproductive syndromes has occurred during the diversification of *Espeletia* as expected in the 'leapfrog' radiation pattern proposed by Chase and Palmer (1997).

**<h1>RESULTS**

**<h2>Phylogenetic inference**

The concatenation of consensus sequence alignments comprised > 4 million bp, including 5.94% of informative sites and 46.59% of ambiguous or missing data. Phylogenetic trees were both well-resolved (96.8% of nodes showed support values > 70% for ML and > 0.95 for BI) and highly congruent with the previous phylogeny of *Espeletia* in Pouchon et al. (2018) (Fig. 2). All intra-specific samples clustered together within the same specific taxon, i.e., *E. purpurascens* Cuatrec., *E. badilloi* Cuatrec., *E. schultzii* Wedd., and *E. tenorae* Aristeg., indicating that the approach developed in Pouchon et al. (2018) and used here appears reliable to estimate phylogenetic relationships at the species level and below. By adding more species in the final dataset, we confirmed all main findings of Pouchon et al. (2018), such as the basal segregation of the genus in two geographically delimited radiations in Colombia and Venezuela, and the evolution in the latter of two clades of trees: *E. trujillensis* Cuatrec. – *E. badilloi*, and *E. spectabilis* Cuatrec. – *E. lucida* Aristeg. (this clade includes the rosette *E. cardonae* Cuatrec.), three clades of monocarpic rosettes: *E. jahnii* Standl.– *E. lopezpalacii* Ruiz-Terán & López-Fig., *E. grisea* Standl.– *E. lindenii* Sch. Bip ex Wedd., and *E. floccosa* Standl. – *E. figueirasii* Cuatrec., and two clades of polycarpic rosettes: *E. angustifolia* Cuatrec. – *E. pannosa* Standl., and *E. thyrsiformis* A.C. Sm. – *E. tenorae*. Some ancient geographical disjunctions suggested in Pouchon et al. (2018) were also confirmed, as for example within the clade of *E. angustifolia* to *E. tenorae*, in which we observed a group of species distributed in the central/northern páramos of the Cordillera de Mérida, i.e., *E. floccosa – E. tenorae* (with the exception of *E. thyrsiformis*), and another with species from the southern páramos, i.e., *E. angustifolia – E. lindenii*. The only sensible topological difference with the previous work consisted in the placement of the clade of trees *E. spectabilis – E. lucida*, which now appears to have diverged earlier in the Venezuelan radiation in comparison to Pouchon et al. (2018).

Divergence time estimations provided relatively narrow age estimates for all nodes except the three most basal ones. The age of the crown node of *Espeletia* was estimated at 2.23 Ma (95% CI: 2.06–2.55 Ma), which is highly consistent with the calibration using the plastid-based age estimation of 2.03–2.56 Ma of Pouchon et al. (2018). The crown age of the Venezuelan clade was estimated at 1.33 Ma (95% CI: 1.20–1.54 Ma), which is 200k years younger than the previous estimate at 1.55 Ma (95% CI: 1.52–1.59 Ma).

**<h2>Patterns of geographic range overlap**

The analysis of geographic range overlap between species' pairs highlighted high levels of sympatry in the studied páramo units (Fig. 3). For example, the average range overlap was estimated as 0.46 for sister-species and as 0.16 for non-sister species ($P < 0.0001$, Appendix S5). Moreover, we observed a decrease in range overlap with increasing divergence times, as illustrated in the Mantel correlogram by a negative correlation between range overlap and recent divergence times, and a null correlation for older divergence times (Fig. 3C).

**<h2>Models of species diversification**

Species diversification models assuming an exponential variation in speciation rates of the Venezuelan clade of *Espeletia* either over time (BDX+T) or in relation to lineage diversity (DDL) appeared as best-fitting models (Fig. 4, Appendix S6). Both the positive α estimate (α = 1.604, Appendix S6) and the plot of the PBX+T model (Appendix S7) reflected a slowdown of speciation rate toward the present. This was concordant with BAMM analyses showing the same exponential decrease in speciation rate over time (Appendix S7). The DDL model indicated that the diversification of species tends to be stabilized at a clade-level carrying capacity K = 56.4, which is quite close to the current estimate of 54 extant species in the clade (Appendix S6). Thus, all three analyses of lineage diversification pointed out a decrease of speciation rates over time.

**<h2>Patterns of traits, climatic niches, and habitats**

The first two PCAmix axes of vegetative traits explained 79% of trait variance among species. The first axis (PC1-VEG, 50% of the variance) discriminated species with tall stems (SH), ramification capacity (STEM), large leaves (LW), and tree growth-form (GF) from others (Fig. 5, Appendix S8a-b). In other words, this axis contrasted rosette vs. tree morphotypes, e.g., *Espeletia neriifolia* (Bonpl. ex Humb.) Sch. Bip. ex Wedd. (Fig. 1C1) vs. *E. figueirasii* (Fig. 1C4). The second axis (PC2-VEG, 29% of the variance) discriminated mainly species with long and wide leaves, such as *E. badilloi* (Fig. 1C6), from species with short and narrow leaves (LL and LW traits), such as *E. nana* Cuatrec. (Fig. 1C8; see Appendix S8a-b,d).

The PCAmix for reproductive traits identified three axes explaining 77% of the variance. Species with large capitula (CD), long ray corollas (RFCL), and long achenes (AL), such as *Espeletia timotensis* (Fig. 1C3) and *E. moritziana* Sch. Bip & Ettingsh. ex Wedd. (Fig. 1C5), were discriminated

from other plants along the first axis (PC1-REP, 38% of the variance, Fig. 5, Appendix S8a-b). The second axis (PC2-REP, 22% of the variance, Fig. 5, Appendix S8a-b,d) distinguished species with terminal inflorescences and low ray/disc flower ratios, such as *E. jabonensis* Cuatrec. (Fig. 1C9), from species with lateral inflorescences and high ray/disc flower ratios, such as *E. timotensis* (Fig. 1C3). Species with long inflorescences (IL), such as *E. figueirasii* (Fig. 1C4), were discriminated from others onto the last axis (PC3-REP, 16% of variance, Appendix S8a-d).

The OMI analyses identified two main climatic gradients explaining over 76% of niche differentiation among species. The first axis (PC1-CLIM, 62% of the variance) is defined by bioclimatic variables related to seasonality in temperature and precipitation regimes (e.g., annual and diurnal range in temperature, or annual precipitation) (Appendix S8a-b). This axis mainly separated species distributed in fluctuating environments in temperatures, with lower precipitation regimes, such as *Espeletia nana* and *E. tenorae*, from species occurring in more stable environments in temperature ranges, with higher precipitation regimes, such as *E. jahnii* and *E. leucactina* Cuatrec. (Appendix S8d). The second axis (PC2-CLIM, 14% of the variance, Appendix S8a-b) separated species typically occurring in high vs. low elevations, e.g., *E. timotensis* vs. *E. griffinii* Ruiz-Terán & López-Fig. (Fig. 5).

For habitats, the two MCA axes of vegetation zonation explained 78% of the habitat variation among species (Appendix S8a-b). The first axis (PC1-HAB, 61% of the variance), distinguished species found in relatively closed habitats at lower ecotones (forest/sub-páramo), such as most trees and a few rosettes (e.g., *Espeletia figueirasii* and *E. marcescens* S.F. Blake), from those occurring in open habitats (proper páramo/super-páramo) (Fig. 5, Appendix S8a-b). The second axis (PC2-HAB, 17% of the variance, Appendix S8a-b) discriminated species found at super-páramo, such as *E. timotensis*, *E. spicata* Sch. Bip ex Wedd., and *E. moritziana*, from those occurring in proper páramos (Fig. 5).

**<h2>Trait-environment correlations**

Regarding vegetative traits, PGLS models indicated a strong positive correlation between PC1-VEG and PC1-HAB axes ($P < 0.001$, Appendix S9a). This means that during the evolution of *Espeletia* the tree morphotype became associated with the forest/sub-páramo and the rosette morphotype with proper páramo/super-páramo (Fig. 5). By investigating separately the quantitative traits that composed the PC1-VEG axis, we found the same correlation between stem height (SH) and habitat (PC1-HAB) ($P <$

0.001, Appendix S9b). For reproductive traits, significant correlations were found between PC1-REP and PC2-CLIM ($P < 0.05$), and between PC1-REP and PC2-HAB ($P < 0.05$) (Appendix S9a). This means that species with larger capitula and larger seeds were found at higher elevations (PC2-CLIM) and in super-páramo (PC2-HAB) (Fig. 5). Investigation of single trait contributing to the reproductive axis indicated a similar correlation between capitulum diameter (CD) and elevation (PC2-CLIM) ($P < 0.005$, Appendix S9b). We did not find significant correlations between other principal components of morphological traits and any other niche or habitat axes.

**<h2>Models of trait evolution**

For the PC1-VEG axis, the Delta model was the best-fitting model with a $\Delta AICc > 3$ in regards with MC (the second best-fit model) and a $\Delta AICc > 4$ with EB (the third best-fit model) (Fig. 6A, see also Appendix S10a for models' parameters). The Delta model was also selected as best-fitting model for the trait stem height (SH) considered alone, with a $\Delta AICc > 2$ in regards with other models (Appendix S10b). For the PC1-REP axis, DD (i.e., DDL and DDX), OU, Delta and BM models had similar statistical support ($\Delta AICc < 2$) (Fig. 6B, Appendix S10a). The same similarity among models of trait evolution was observed for the capitulum diameter (CD) separately (Appendix S10b). The ensemble of these results leads to uncertainty regarding the best evolutionary model applicable to reproductive traits.

Finally, we found contrasted estimates of the Pagel's delta for the two main axes of vegetative and reproductive traits ($\delta = 0.174$ for PC1-VEG and $\delta = 2.543$ for PC1-REP), indicating that vegetative morphotypes diversified earlier than reproductive traits during the evolutionary history of the Venezuelan clade of *Espeletia* (Fig. 7). A similar difference in Pagel's delta was observed between single traits contributing significantly to PC1-VEG and PC1-REP axes, i.e., $\delta = 0.282$ for stem height (SH) and $\delta = 1.684$ for capitulum diameter (CD) (Appendix S10).

**<h1>DISCUSSION**

In this work we used whole genome shotgun sequencing to perform a comparative analysis of ecological and species diversification in *Espeletia*, a genus that has long been acclaimed as a paradigmatic example of adaptive radiation in páramos (Monasterio and Sarmiento, 1991). Our analysis provides a more complete phylogeny of *Espeletia*, including novel insights into the phylogenetic placement of several species that had remained unstudied until now. But more importantly, our study provides a compelling example of the ecological processes that drove the

explosive plant radiations documented in several lineages of tropical high-elevation regions (Madriñán et al., 2013; Hughes and Atchison, 2015).

**<h2>Phylogenetic signatures of ecological divergence in *Espeletia***

The high diversification rates that gave rise to the rich flora of páramos has traditionally been assigned to geographic isolation driven by the combined action of Andean uplift and the climatic cycles (Antonelli and Sanmartín, 2011; Flantua et al., 2019). In *Espeletia*, allopatry was shown as a predominant driver of speciation for Colombian lineages (Diazgranados and Barber, 2017; Padilla-González et al., 2017; Cortés et al., 2018) and that isolation-by-environment tends to mask isolation-by-distance (Cortés et al., 2018). Our results indeed suggest that some degree of allopatry drove early lineage split in the Venezuelan clade of *Espeletia*, as exampled by some geographic disjunctions observed at deeper nodes of the phylogeny. Nevertheless, our results also show a strong and significant sympatric build-up of closely related species, which tend to co-occur in the same páramo units. Even more interesting, we found that this rate of sympatry tends to decrease over time after speciation, which is a geographical pattern expected under a scenario of sympatric speciation (Pigot and Tobias, 2013). This suggests that sympatric speciation may have been an important mode of speciation within the Venezuelan clade of *Espeletia*, although some degree of spatial isolation within páramos may still have helped drive reproductive isolation between closely related species.

Past climatic dynamics, considered as a proxy for past contraction and expansion of high-elevation biotas, do not seem to have had a significant effect on the diversification dynamics of the Venezuelan clade of *Espeletia*, contrary to recent evidence in Chinese *Primulina* Hance [Gesneriaceae] (Kong et al., 2017), or Andean Lobelioideae [Campanulaceae] (Lagomarsino et al., 2016) and *Lupinus* (Nevado et al., 2018). Instead, diversification models show that speciation rates in *Espeletia* appear time- and diversity-dependent, decreasing as species accumulate towards a clade-level carrying capacity close to the known extant number of species in this group. Indeed, both PBX+T and DDL diversification models converged to the same conclusion in regards with a slowdown of speciation rate through time, a trend also recovered with the BAMM analysis. This agrees with Burin et al. (2019) who showed that both PBX+T and BAMM models estimate well the slowdown in diversity dynamics expected when speciation rate declines with time. Such a slowdown in diversification rates could be interpreted by a saturation of the ecological space with niche differentiation (Rabosky, 2009; Nuismer and Harmon, 2015), but also by either a reduction of vicariance events as species' ranges tend to shrink (Moen and Morlon, 2014) or by a lowering of extrinsic factors (e.g., in rate of environmental and

geological changes) causing vicariance (Rundell and Price, 2009). Although Etienne et al. (2016) have shown that estimates of clade-level carrying capacity could be biased in clades that are young or subjected to high rates of extinction, so that results that depend on this parameter must be interpreted with caution, the high degree of sympatry observed here between recently diverged species, along with additional results on trait and niche evolution (see paragraphs below) make the existence of ecological limits as species accumulated within páramos rather likely.

The study of trait evolution provides further insights into the ecological drivers of speciation in the Venezuelan clade of *Espeletia*. We showed that sets of vegetative or reproductive traits seem to have respectively diversified and converged in relation to a variety of ecological niches corresponding to environmental gradients typically occurring within páramos. This is illustrated in this study by the significant phylogenetic correlations between species trait combinations and niches (i.e., climate, habitat), leading to adaptive syndromes for both vegetative and reproductive traits. A first axis of adaptation seems to be associated with the ecotone between closed vegetation (i.e., forest and subpáramo) and open vegetation (i.e., proper páramo), along which different lineages have repeatedly differentiated for some vegetative traits corresponding to tree and rosette morphotypes, respectively. Species occurring in lower elevations and closed habitats typically display a trait syndrome implying taller and branched stems, and larger leaves disposed more loosely around the apical meristem. Such correlation was also found for single trait analyses of stem height. This trend is supported both by the numerous adaptive values provided by these two morphotypes in their respective habitats (Baruch and Smith, 1979; Smith, 1981; Monasterio and Sarmiento, 1991), and by the numerous transitions in herbaceaous/rosettes vs. woody growth forms associated with open/closed habitats found in Andean taxa, e.g., *Valeriana* L. [Valerianaceae], *Gentianella* Moench [Gentianaceae], and *Loricaria* Wedd. [Asteraceae] (Sklenář et al., 2011; Kolář et al., 2016), and *Senecio* L. [Asteraceae] (Dušková et al., 2017). Another axis of adaptation along environmental gradients concerned reproductive traits, with the emergence of a trait syndrome implying larger capitula, corollas, and achenes in some lineages occurring at higher elevations and/or in super-páramo habitats. Such correlation was also shown for the capitulum diameter alone, independently from other reproductive traits. As noted by Cuatrecasas (2013), high-elevation *Espeletia* plants typically develop inflorescences with fewer but larger drooping to pendulous capitula with thickly lanate involucres, greater flower number, and longer flowering period. Such a transition in capitulum morphology very likely represents an adaptive shift from insect to wind pollination, likely due to a lower pollinator availability at high elevations in the Andes (Berry and Calvo, 1989, 1994; Fagua and Gonzalez, 2007). On the other hand, some of the reproductive trait

shifts could also confer flower protection against snow or daily frosts at higher elevations (Sklenář, 1999; Cuatrecasas, 2013).

Our study further suggests that the evolutionary trajectories of vegetative and reproductive trait syndromes seem to have been driven by species' interactions within páramos. The main axis of vegetative differentiation and the stem height alone, both associated with habitat segregation within páramos, show a clear pattern of diversification slow-down overtime, illustrated by the choice of Delta as the best-fitting model of trait evolution. Indeed, a $\delta < 1$ for this model suggests that vegetative morphotypes have rapidly diversified during the radiation of *Espeletia* species, with a slowdown towards the present, as would be expected under an 'early-burst' evolutionary scenario (Pagel, 1999). Moreover, the next choice models (MC, a competition model, and EB, a time-dependent model), imply a diversity-dependence pattern. Indeed, matching competition models such as MC explicitly account for species' interactions in comparison to time-dependent models such as EB, in which time can be viewed as a proxy of niche saturation (Drury et al., 2016; Aristide and Morlon, 2019). All these models suggest a slowdown of phenotypic evolution in vegetative morphotypes as species accumulate and fill trait space (Weir and Mursleen, 2013; Drury et al., 2018). This evolutionary dynamic provides further support to the ecological divergence processes highlighted above by the diversity-dependent pattern in lineage diversification and is compatible with a scenario of divergent vegetative trait evolution bounded by interspecific competition, as expected in adaptive radiations (Rabosky, 2009; Nuismer and Harmon, 2015).

Compared with vegetative traits, both the main axis of reproductive differentiation, or the capitulum diameter alone, show less clear-cut results, as DD, OU, Delta, and BM models had similar AICc values ($dAICc < 2$). As a result, there remain some strong uncertainties in the evolutionary trajectory and the ecological factors that drove the diversification of reproductive morphology in *Espeletia*.

**<h2>Sequential and leapfrog adaptive radiation in *Espeletia***

Our analyses showed that the main axes of trait variation along which different lineages in the Venezuelan clade of *Espeletia* have consistently diverged are associated with the main environmental gradients of the páramos (i.e., macro-habitats given by PC-HAB axes). All this supports a model of adaptive divergence proceeding along sequential axes of habitats, in which divergence in traits correlating to higher levels of resources precedes divergence of traits correlating to lower niche levels

(i.e., micro-habitats) (Gavrilets and Losos, 2009). With the ample intra- and inter-specific evidence confirming the adaptive value of many other traits in *Espeletia*, e.g., pubescence (Baruch and Smith, 1979; Meinzer et al., 1985), pith volume (Goldstein et al., 1984; Meinzer et al., 1985), or supercooling (Goldstein et al., 1985; Rada et al., 1985), together with evidence of species distribution along fine-scale environmental gradients in regards with soil moisture, grain size, and ground slope (Smith, 1981; Monasterio and Sarmiento, 1991; Pérez, 1996; see Appendix S11), it is legitimate to posit that a large part of the dazzling morphological diversity in the Venezuelan clade of *Espeletia* is also attributable to the same divergent selective pressures that have driven the evolution of a wealth of particular traits in varied micro-environments of the páramos.

We showed that the differentiation of vegetative and reproductive traits combinations diverging among *Espeletia* species at this macro-habitat scale also occurred at different periods of time. Indeed, estimated values of Pagel's delta demonstrate that the evolution of vegetative morphotypes occurred earlier in the phylogenetic tree of *Espeletia* than the evolution of reproductive morphotypes, which is mostly concentrated in recent branches of the tree. The difference in the tempo of evolution of vegetative and reproductive trait syndromes is consistent with Grant's divergence rule for flowering plants (1949), for whom diversification of vegetative traits should have occurred earlier than reproductive ones in plant clades pollinated by abiotic agents (e.g., wind or water) and generalist biotic pollinators, which is the case in *Espeletia* (Berry and Calvo, 1989, 1994; Fagua and Gonzalez 2007). Our results are also clearly in line with the idea of leapfrog adaptive radiation (Chase and Palmer, 1997), stipulating that the acquisition of particular vegetative traits should allow lineages to colonize a new adaptive zone related to particular habitats, followed by the acquisition of secondary reproductive traits (e.g., pollination, dispersal syndromes), allowing to evolve to novel biotic interactions within these new habitats. This pattern was originally described in the orchid subtribe Oncidiinae (Chase and Palmer, 1997) and recently evoked in New Caledonian *Oxera* [Lamiaceae] (Barrabé et al., 2019). Here, we provided a further example of such pattern, this time in a high-elevation plant radiation.

## <h1>CONCLUSIONS

Our study shows that the radiation of *Espeletia* in the Venezuelan páramos depicts compelling phylogenetic signatures of ecological divergence within these habitats. The evolutionary scenario proposed here suggests that species diversify in a macro-evolutionary adaptive landscape (sensu Simpson, 1944). This mode of phenotypic evolution has been proposed in some animal radiations, e.g., *Anolis* Daudin lizards of the Greater Antilles (Mahler et al., 2013), or the African Cichlid fish (Aguilée

et al., 2012; Brawand et al., 2014; Malinsky et al., 2018). Among plants, evidence for adaptive radiations has emerged in American Asclepiadinae (Agrawal et al., 2009), Hawaiian lobelioids (Givnish et al., 2009), Hawaiian silverswords alliance (Baldwin and Wagner, 2010; Blonder et al., 2016), as well as in other island or mountain taxa (recently reviewed in Nevado et al., 2019). In páramo taxa, adaptive radiations have been shown in *Lupinus* (Drummond et al., 2012b; Nevado et al., 2016), *Calceolaria* L. [Calceolariaceae] and *Puya* Molina [Bromeliaceae\ (Nevado et al., 2019), and envisioned in Colombian *Espeletia* (Cortés et al., 2018). As a whole, our results suggest great levels of sympatry and diversity dependence patterns in traits and lineages diversification, and highly support phylogenetic predictions of ecological and adaptive divergence during the radiation of *Espeletia* in the Venezuelan páramos. This reinforces the idea that ecological and adaptive divergences are prevalent in plant radiations from oceanic and sky island ecosystems (Nevado et al., 2019). Furthermore, this study provides support to the idea that rapid diversification does not depend on single factors but results from the combined action of biotic and abiotic factors, making sense with previous conceptual (Bouchenak- Khelladi et al., 2015; Donoghue and Sanderson, 2015) and empirical studies (Lagomarsino et al., 2016; Ebersbach et al., 2017; Condamine et al., 2018; Cortés et al., 2018). Besides, the radiation of *Espeletia* seems dependent on ecological opportunities occurring at different temporal scales, which have probably been progressively filled up by species diversifying mostly through pervasive ecological speciation, with different selection pressures operating in a leapfrog fashion over time.

This study also opens new perspectives to fully determine adaptive processes leading to speciation in *Espeletia* from phylogenetic data and other genomic approaches. Indeed, it could be interesting to simulate phylogenetic trees with different trait evolutionary scenarios (e.g., assuming diversity- or time-dependency) to check whether complex models could be spuriously retrieved as best-fitting models (Pyron and Burbrink, 2013; Drury et al., 2016). Moreover, it could also be interesting to perform additional approaches to model species' interactions while incorporating the geographical overlap between species or ancestral lineages (Drury et al., 2016, 2018; Harmon et al., 2019). This could provide a bio-geographical context to scenarios of trait evolution, and help further assessment of the role of species' interactions during the evolution of this plant group. Such overlap could be estimated through species distribution modeling, which has only been implemented so far in 28 Venezuelan *Espeletia* species (Mavárez et al., 2019). Furthermore, alternative genomic approaches to phylogenetic reconstruction (i.e., genome-wide studies) could be considered to clearly determine adaptive processes in evolutionary radiations, as it was shown from transcriptomic or whole-genome

sequencing data in plants' (Nevado et al., 2016, 2019) and animals' radiations (Brawand et al., 2014; Cornetti et al., 2015; Malinsky et al., 2018). Such approaches have remained rare so far but applied to this case would permit to assess the correlation between the frequency of adaptive evolution of genomes in *Espeletia*, the ecological space occupied by species and the rate of lineage and trait diversification, which is expected to be positive under a scenario of adaptive radiation (Nevado et al., 2019).

## <h1>ACKNOWLEDGMENTS

We would like to dedicate this article to the memory of Serge Aubert (1966-2015), our friend and colleague, without whom all this work would not have been possible. We thank Université Grenoble Alpes, Centre National de la Recherche Scientifique (PEPS and OSUG grants), and the ANR project Origin-Alps (ANR-16-CE93-0004) for financial support. We are also grateful to the Venezuelan Oficina Nacional de Diversidad Biológica and the Instituto Nacional de Parques for their help with collecting permits. Luis "Kicke" Gámez, Reina Gonto, Jafet M. Nassar, John Parra, and Thibaud Syre for help during fieldwork, and Centro de Investigaciones de Astronomía, Dirección Regional Inparques Mérida and Teleférico Mukumbarí for help with logistics. We thank the AEEM technical platform of LECA for genomic analyses. Bioinformatic computations were performed using the CIMENT infrastructure, which is supported by the Rhône-Alpes region (GRANT CPER07_13 CIRA). We received help from Jonathan Drury and Florian Boucher with statistical analyses, Anne-Sophie Quatela with morphological trait acquisition, Fred Boyer with bioinformatics, and Nadir Alvarez, Jérôme Chave, Thomas Haevermans, and two anonymous reviewers with an earlier version of this manuscript. This work is part of Charles Pouchon's Ph.D. dissertation at the Université Grenoble Alpes.

## <h1>AUTHOR CONTRIBUTIONS

C.P., S.L., and J.M. designed the study; A.F., S.A., and J.M. collected samples; A.A. performed shotgun library preparation and sequencing; C.P. performed bioinformatics and phylogenetic analyses; C.P. and S.L. analyzed the data and performed diversification analyses; C.P. wrote the text with contributions from all co-authors.

## <h1>DATA AVAILABILITY

Sequence data have been deposited at the European Nucleotide Archive (ERP123990). Alignment, phylogenetic trees and traits coordinates are available from the Dryad Digital Repository: https://doi.org/10.5061/dryad.cvdncjt2p (Pouchon et al., 2020).

## <h1> SUPPORTING INFORMATIONS

Additional Supporting Information may be found online in the supporting information document for this article.

**APPENDIX S1.** Sampling and shotgun libraries preparation.

**APPENDIX S2a.** Bioinformatic pipeline of nuclear genomic regions reconstructions.

**APPENDIX S2b.** Summary statistics over sequencing and phylogenetic alignments.

**APPENDIX S3.** Table summarizing the distribution of species into the main páramo units.

**APPENDIX S4.** Estimation of speciation rates through time under BAMM model.

**APPENDIX S5.** Comparison of geographic range overlap between sister and non-sister species.

**APPENDIX S6.** Table summarizing the estimates of lineages diversification model.

**APPENDIX S7.** Variation of speciation rate through time of the Venezuelan clade of *Espeletia*.

**APPENDIX S8a.** Contribution of habitat (HAB) and climatic (CLIM) variables into the environmental space, and of vegetative (VEG) and reproductive (REP) trait into the morphological space.

**APPENDIX S8b.** Distribution of species into the first two axes of the (a.) environmental and (b.) morphological space.

**APPENDIX S8c.** Projection of reproductive space occupied by species for the first (PC1-REP) and the third component (PC3-REP).

**APPENDIX S8d.** Phylogenetic projection of morphological (PC2-VEG, PC2-REP, PC3-REP) and environmental (PC1-CLIM) space occupied by species.

**APPENDIX S9a.** Phylogenetic generalized least-squares (PGLS) models assessing the relationship between the Environmental and the morphological space position occupied by species.

**APPENDIX S9b.** Phylogenetic generalized least-squares (PGLS) models assessing the relationship between the Environmental space position occupied by species and quantitative traits composing the vegetative (PC1-VEG) and the reproductive (PC1-REP) components.

**APPENDIX S10a.** Fitted models of trait evolution explored for PC1-VEG and PC1-REP morphological components.

**APPENDIX S10b.** Fitted models of trait evolution explored two traits independently correlating to environment: stem height (SH) and the capitulum diameter (CD).

**APPENDIX S11.** Assembly of *Espeletia* communities in the páramo of Piedras Blancas (Venezuela) according to ecological preferences of species according to moisture and slope.

**<h1>LITERATURE CITED**

Aberer, A. J., K. Kobert, and A. Stamatakis. 2014. ExaBayes: Massively parallel bayesian tree inference for the whole-genome era. *Molecular Biology and Evolution* 31: 2553–2556.

Agrawal, A. A., M. Fishbein, R. Halitschke, A. P. Hastings, D. L. Rabosky, and S. Rasmann. 2009. Evidence for adaptive radiation from a phylogenetic study of plant defenses. *Proceedings of the National Academy of Sciences, USA* 106: 18067–18072.

Aguilée, R., D. Claessen, and A. Lambert. 2012. Adaptive radiation driven by the interplay of eco-evolutionary and landscape dynamics. *Evolution* 67: 1291–1306.

Antonelli, A., and I. Sanmartín. 2011. Why are there so many plant species in the Neotropics? *Taxon* 60: 403–414.

Aristide, L., and H. Morlon. 2019. Understanding the effect of competition during evolutionary radiations: An integrated model of phenotypic and species diversification. *Ecology Letters* 22: 2006–2017.

Baldwin, B. G., and W. L. Wagner. 2010. Hawaiian angiosperm radiations of North American origin. *Annals of Botany* 105: 849–879.

Barrabé, L., S. Lavergne, G. Karnadi-Abdelkader, B. T. Drew, P. Birnbaum, and G. Gâteblé. 2019. Changing ecological opportunities facilitated the explosive diversification of New Caledonian *Oxera* (Lamiaceae). *Systematic Biology* 68: 460–481.

Baruch, Z., and A. P. Smith. 1979. Morphological and physiological correlates of niche breadth in two species of *Espeletia* (Compositae) in the Venezuelan Andes. *Oecologia* 38: 71–82.

Benjamini, Y., and Y. Hochberg. 1995. Controlling the false discovery rate: A practical and powerful approach to multiple testing. *Journal of the Royal Statistical Society, B (Methodological)* 57: 289–300.

Berry, P. E., and R. N. Calvo. 1989. Wind pollination, self-incompatibility, and altitudinal shifts in pollination systems in the High Andean genus *Espeletia* (Asteraceae). *American Journal of Botany* 76: 1602–1614.

Berry, P. E., and R. N. Calvo. 1994. An overview of the reproductive biology of *Espeletia* (Asteraceae) in the Venezuelan Andes. *In* P. W. Rundel, A. P. Smith, and F. C. Meinzer [eds.], Tropical alpine environments, 229–248. Cambridge University Press, Cambridge, UK.

Blonder, B., B. G. Baldwin, B. J. Enquist, and R. H. Robichaux. 2016. Variation and macroevolution in leaf functional traits in the Hawaiian silversword alliance (Asteraceae). *Journal of Ecology* 104: 219–228.

Bouchenak-Khelladi, Y., R. E. Onstein, Y. Xing, O. Schwery, and H. P. Linder. 2015. On the complexity of triggering evolutionary radiations. *New Phytologist* 207: 313–326.

Boucher, F. C., S. Lavergne, M. Basile, P. Choler, and S. Aubert. 2016. Evolution and biogeography of the cushion life form in angiosperms. *Perspectives in Plant Ecology, Evolution and Systematics* 20: 22–31.

Boucher, F. C., N. E. Zimmermann, and E. Conti. 2016. Allopatric speciation with little niche divergence is common among alpine Primulaceae. *Journal of Biogeography* 43: 591–602.

Brawand, D., C. E. Wagner, Y. I. Li, M. Malinsky, I. Keller, S. Fan, O. Simakov, et al. 2014. The genomic substrate for adaptive radiation in African cichlid fish. *Nature* 513: 375–381.

Brown, G. K., G. Nelson, and P. Y. Ladiges. 2006. Historical biogeography of *Rhododendron* section *Vireya* and the Malesian Archipelago. *Journal of Biogeography* 33: 1929–1944.

Burin, G., L. R. V. Alencar, J. Chang, M. E. Alfaro, and T. B. Quental. 2019. How well can we estimate diversity dynamics for clades in diversity decline? *Systematic Biology* 68: 47–62.

Burnham, K. P., and D. R. Anderson. 2002. Model selection and multimodel inference: A practical information-theoretic approach, 2nd ed. Springer-Verlag, New York, NY, USA.

Chase, M. W., and J. D. Palmer. 1997. Leapfrog radiation in floral and vegetative traits among twig epiphytes in the orchid subtribe Oncidiinae. *In* T. J. Givnish and K. J. Sytsma [eds.], Molecular evolution and adaptive radiation, 331–352. Cambridge University Press, Cambridge, UK.

Condamine, F. L., J. Rolland, S. Höhna, F. A. H. Sperling, and I. Sanmartín. 2018. Testing the role of the red queen and court jester as drivers of the macroevolution of Apollo butterflies. *Systematic Biology* 67: 940–964.

Cornetti, L., L. M. Valente, L. T. Dunning, X. Quan, R. A. Black, O. Hébert, and V. Savolainen. 2015. The genome of the "Great Speciator" provides insights into bird diversification. *Genome Biology and Evolution* 7: 2680–2691.

Cortés, A. J., L. N. Garzón, J. B. Valencia, and S. Madriñán. 2018. On the causes of rapid diversification in the páramos: Isolation by ecology and genomic divergence in *Espeletia*. *Frontiers in Plant Science* 9: Article 1700.

Cuatrecasas, J. 2013. A systematic study of the subtribe Espeletiinae: Heliantheae. Asteraceae. Memoirs of the New York Botanical Garden, vol. 107. New York Botanical Garden Press, Bronx, NY, USA.

Diazgranados, M. 2012. A nomenclator for the frailejones (Espeletiinae Cuatrec., Asteraceae). *PhytoKeys* 16: 1–52.

Diazgranados, M., and J. C. Barber. 2017. Geography shapes the phylogeny of frailejones (Espeletiinae Cuatrec., Asteraceae): A remarkable example of recent rapid radiation in sky islands. *PeerJ* 5: e2698.

Dolédec, S., D. Chessel, and C. Gimaret-Carpentier. 2000. Niche separation in community analysis: A new method. *Ecology* 81: 2914–2927.

Donoghue, M. J., and M. J. Sanderson. 2015. Confluence, synnovation, and depauperons in plant diversification. *New Phytologist* 207: 260–274.

Dray, S., and A.-B. Dufour. 2007. The ade4 package: Implementing the duality diagram for ecologists. *Journal of Statistical Software* 22: 1–20.

Drummond, A. J., M. A. Suchard, D. Xie, and A. Rambaut. 2012. Bayesian phylogenetics with BEAUti and the BEAST 1.7. *Molecular Biology and Evolution* 29: 1969–1973.

Drummond, C. S. 2008. Diversification of *Lupinus* (Leguminosae) in the western New World: Derived evolution of perennial life history and colonization of montane habitats. *Molecular Phylogenetics and Evolution* 48: 408–421.

Drummond, C. S., R. J. Eastwood, S. T. S. Miotto, and C. E. Hughes. 2012. Multiple continental radiations and correlates of diversification in *Lupinus* (Leguminosae): Testing for key innovation with incomplete taxon sampling. *Systematic Biology* 61: 443–460.

Drury, J., J. Clavel, M. Manceau, and H. Morlon. 2016. Estimating the effect of competition on trait evolution using maximum likelihood inference. *Systematic Biology* 65: 700–710.

Drury, J. P., J. A. Tobias, K. J. Burns, N. A. Mason, A. J. Shultz, and H. Morlon. 2018. Contrasting impacts of competition on ecological and social trait evolution in songbirds. *PLoS Biology* 16: e2003563.

Dušková, E., P. Sklenář, F. Kolář, D. L. A. Vásquez, K. Romoleroux, T. Fér, and K. Marhold. 2017. Growth form evolution and hybridization in *Senecio* (Asteraceae) from the high equatorial Andes. *Ecology and Evolution* 7: 6455–6468.

Ebersbach, J., J. Schnitzler, A. Favre, and A. N. Muellner-Riehl. 2017. Evolutionary radiations in the species-rich mountain genus *Saxifraga* L. *BMC Evolutionary Biology* 17: 119.

Etienne, R. S., H. Morlon, and A. Lambert. 2012. Estimating the duration of speciation from phylogenies. *Evolution* 68: 2430–2440.

Etienne, R. S., A. L. Pigot, and A. B. Phillimore. 2016. How reliably can we infer diversity-dependent diversification from phylogenies? *Methods in Ecology and Evolution* 7: 1092–1099.

Fagua, J. C., and V. H. Gonzalez. 2007. Growth rates, reproductive phenology, and pollination ecology of *Espeletia grandiflora* (Asteraceae), a giant Andean caulescent rosette. *Plant Biology* 9: 127–135.

Fick, S. E., and R. J. Hijmans. 2017. Worldclim 2: New 1-km spatial resolution climate surfaces for global land areas. *International Journal of Climatology* 37: 4302–4315.

Flantua, S. G. A., A. O'Dea, R. E. Onstein, C. Giraldo, and H. Hooghiemstra. 2019. The flickering connectivity system of the north Andean páramos. *Journal of Biogeography* 46: 1808–1825.

Gamisch, A. 2020. Technical comment on Condamine et al. (2019): A cautionary note for users of linear diversification dependencies. *Ecology Letters* 23: 1169–1171.

Gavrilets, S., and J. B. Losos. 2009. Adaptive radiation: Contrasting theory with data. *Science* 323: 732–737.

Givnish, T. J. 2015. Adaptive radiation versus 'radiation' and 'explosive diversification': Why conceptual distinctions are fundamental to understanding evolution. *New Phytologist* 207: 297–303.

Givnish, T. J., K. C. Millam, A. R. Mast, T. B. Paterson, T. J. Theim, A. L. Hipp, J. M. Henss, et al. 2009. Origin, adaptive radiation and diversification of the Hawaiian lobeliads (Asterales: Campanulaceae). *Proceedings of the Royal Society of London, B, Biological Sciences* 276: 407–416.

Glor, R. E. 2010. Phylogenetic insights on adaptive radiation. *Annual Review of Ecology, Evolution, and Systematics* 41: 251–270.

Goldstein, G., F. Meinzer, and M. Monasterio. 1984. The role of capacitance in the water balance of Andean giant rosette species. *Plant, Cell & Environment* 7: 179–186.

Goldstein, G., F. Rada, and A. Azocar. 1985. Cold hardiness and supercooling along an altitudinal gradient in Andean giant rosette species. *Oecologia* 68: 147–152.

Grant, V. 1949. Pollination systems as isolating mechanisms in Angiosperms. *Evolution* 3: 82–97.

Gregory-Wodzicki, K. M. 2000. Uplift history of the central and northern Andes: A review. *GSA Bulletin* 112: 1091–1105.

Harmon, L. J., C. S. Andreazzi, F. Débarre, J. Drury, E. E. Goldberg, A. B. Martins, C. J. Melián, et al. 2019. Detecting the macroevolutionary signal of species interactions. *Journal of Evolutionary Biology* 32: 769–782.

Harmon, L. J., J. B. Losos, T. Jonathan Davies, R. G. Gillespie, J. L. Gittleman, W. Bryan Jennings, K. H. Kozak, et al. 2010. Early bursts of body size and shape evolution are rare in comparative data. *Evolution* 64: 2385–2396.

Harmon, L. J., J. T. Weir, C. D. Brock, R. E. Glor, and W. Challenger. 2008. GEIGER: Investigating evolutionary radiations. *Bioinformatics* 24: 129–131.

Hofstede, R., P. Segarra, P. Mena-Vásconez [eds.]. 2003. Los páramos del mundo: Proyecto atlas mundial de los páramos. Global Peatland Initiative/NC-IUCN/ Ecociencia, Quito, Ecuador.

Hooghiemstra, H., V. M. Wijninga, and A. M. Cleef. 2006. The paleobotanical record of Colombia: Implications for biogeography and biodiversity. *Annals of the Missouri Botanical Garden* 93: 297–325.

Hughes, C. E., and G. W. Atchison. 2015. The ubiquity of alpine plant radiations: From the Andes to the Hengduan Mountains. *New Phytologist* 207: 275–282.

Joly, S., P. B. Heenan, and P. J. Lockhart. 2014. Species radiation by niche shifts in New Zealand's rockcresses (*Pachycladon*, Brassicaceae). *Systematic Biology* 63: 192–202.

Kolář, F., E. Dušková, and P. Sklenář. 2016. Niche shifts and range expansions along cordilleras drove diversification in a high-elevation endemic plant genus in the tropical Andes. *Molecular Ecology* 25: 4593–4610.

Kong, H., F. L. Condamine, A. J. Harris, J. Chen, B. Pan, M. Möller, V. S. Hoang, and M. Kang. 2017. Both temperature fluctuations and East Asian monsoons have driven plant diversification in the karst ecosystems from southern China. *Molecular Ecology* 26: 6414–6429.

Lagomarsino, L. P., F. L. Condamine, A. Antonelli, A. Mulch, and C. C. Davis. 2016. The abiotic and biotic drivers of rapid diversification in Andean bellflowers (Campanulaceae). *New Phytologist* 210: 1430–1442.

Lagomarsino, L. P., E. J. Forrestel, N. Muchhala, and C. C. Davis. 2017. Repeated evolution of vertebrate pollination syndromes in a recently diverged Andean plant clade. *Evolution* 71: 1970–1985.

Li, H., and R. Durbin. 2009. Fast and accurate short read alignment with Burrows-Wheeler transform. *Bioinformatics* 25: 1754–1760.

Li, H., B. Handsaker, A. Wysoker, T. Fennell, J. Ruan, N. Homer, G. Marth, et al. 2009. The sequence alignment/map format and SAMtools. *Bioinformatics* 25: 2078–2079.

Luteyn, J. L. 1999. Páramos: A checklist of plant diversity, geographical distribution, and botanical literature. New York Botanical Garden Press, Bronx, NY, USA.

Madriñán, S., A. J. Cortés, and J. E. Richardson. 2013. Páramo is the world's fastest evolving and coolest biodiversity hotspot. *Frontiers in Genetics* 4: 192.

Mahler, D. L., T. Ingram, L. J. Revell, and J. B. Losos. 2013. Exceptional convergence on the macroevolutionary landscape in island lizard radiations. *Science* 341: 292–295.

Malinsky, M., H. Svardal, A. M. Tyers, E. A. Miska, M. J. Genner, G. F. Turner, and R. Durbin. 2017. Whole genome sequences of Malawi cichlids reveal multiple radiations interconnected by gene flow. *Nature Ecology & Evolution* 2: 1940–1955.

Mavárez, J. 2019. A taxonomic revision of *Espeletia* (Asteraceae). The Venezuelan radiation. *Harvard Papers in Botany* 24: 131–244.

Mavárez, J., S. Bézy, T. Goeury, A. Fernández, and S. Aubert. 2019. Current and future distributions of Espeletiinae (Asteraceae) in the Venezuelan Andes based on statistical downscaling of climatic variables and niche modelling. *Plant Ecology & Diversity* 12: 633–647.

Meinzer, F. C., G. H. Goldstein, and P. W. Rundel. 1985. Morphological changes along an altitude gradient and their consequences for an Andean giant rosette plant. *Oecologia* 65: 278–283.

Moen, D., and H. Morlon. 2014. Why does diversification slow down? *Trends in Ecology & Evolution* 29: 190–197.

Monasterio, M., and L. Sarmiento. 1991. Adaptive radiation of *Espeletia* in the cold Andean tropics. *Trends in Ecology & Evolution* 6: 387–391.

Morlon, H., E. Lewitus, F. L. Condamine, M. Manceau, J. Clavel, and J. Drury. 2016. RPANDA: An R package for macroevolutionary analyses on phylogenetic trees. *Methods in Ecology and Evolution* 7: 589–597.

Morlon, H., T. L. Parsons, and J. B. Plotkin. 2011. Reconciling molecular phylogenies with the fossil record. *Proceedings of the National Academy of Sciences, USA* 108: 16327–16332.

Nevado, B., G. W. Atchison, C. E. Hughes, and D. A. Filatov. 2016. Widespread adaptive evolution during repeated evolutionary radiations in New World lupins. *Nature Communications* 7: 12384.

Nevado, B., N. Contreras- Ortiz, C. Hughes, and D. A. Filatov. 2018. Pleistocene glacial cycles drive isolation, gene flow and speciation in the high-elevation Andes. *New Phytologist* 219: 779–793.

Nevado, B., E. L. Y. Wong, O. G. Osborne, and D. A. Filatov. 2019. Adaptive evolution is common in rapid evolutionary radiations. *Current Biology* 29: 3081–3086.

Nuismer, S. L., and L. J. Harmon. 2015. Predicting rates of interspecific interaction from phylogenetic trees. *Ecology Letters* 18: 17–27.

Nürk, N. M., G. W. Atchison, and C. E. Hughes. 2019. Island woodiness underpins accelerated disparification in plant radiations. *New Phytologist* 224: 518–531

Nürk, N. M., C. Scheriau, and S. Madriñán. 2013. Explosive radiation in high Andean *Hypericum*—rates of diversification among New World lineages. *Frontiers in Genetics* 4: 175.

Oksanen, J., F. G. Blanchet, M. Friendly, R. Kindt, P. Legendre, D. McGlinn, P. R. Minchin, et al. 2018. vegan: Community ecology package. R package version 2.5-2. Website: https://CRAN.R-project.org/package=vegan.

Orme, D., R. Freckleton, G. Thomas, T. Petzoldt, S. Fritz, N. Isaac, and W. Pearse. 2018. caper: Comparative analyses of phylogenetics and evolution in R. version 1.0.1. Website: https://cran.r-project.org/web/packages/caper/index.html

Padilla-González, G. F., M. Diazgranados, and F. B. D. Costa. 2017. Biogeography shaped the metabolome of the genus *Espeletia* : A phytochemical perspective on an Andean adaptive radiation. *Scientific Reports* 7: 8835.

Pagel, M. 1999. Inferring the historical patterns of biological evolution. *Nature* 401: 877–884.

Paradis, E., S. Blomberg, B. Bolker, J. Brown, S. Claramunt, J. Claude, et al. 2020. Package "ape": Analyses of phylogenetics and evolution, version 5.4-1. Website: https://cran.r-project.org/web/packages/ape/.

Pérez, F. L. 1996. The effects of giant Andean rosettes on surface soils along a high paramo toposequence. *GeoJournal* 40: 283–298.

Pigot, A. L., and J. A. Tobias. 2013. Species interactions constrain geographic range expansion over evolutionary time. *Ecology Letters* 16: 330–338.

Pouchon, C., A. Fernández, J. M. Nassar, F. Boyer, S. Aubert, S. Lavergne, and J. Mavárez. 2018. Phylogenomic analysis of the explosive adaptive radiation of the *Espeletia* complex (Asteraceae) in the tropical Andes. *Systematic Biology* 67: 1041–1060.

Pouchon, C., S. Lavergne, Á. Fernández, A. Alberti, S. Aubert, and Jesús Mavárez. 2020. Data from: Phylogenetic signatures of ecological divergence and leapfrog adaptive radiation in *Espeletia*. Dryad Digital Repository: https://doi.org/10.5061/dryad.cvdncjt2p.

Price, T. D., D. M. Hooper, C. D. Buchanan, U. S. Johansson, D. T. Tietze, P. Alström, U. Olsson, et al. 2014. Niche filling slows the diversification of Himalayan songbirds. *Nature* 509: 222–225.

Pyron, R. A., and F. T. Burbrink. 2013. Phylogenetic estimates of speciation and extinction rates for testing ecological and evolutionary hypotheses. *Trends in Ecology & Evolution* 28: 729–736.

Rabosky, D. L. 2009. Ecological limits and diversification rate: Alternative paradigms to explain the variation in species richness among clades and regions. *Ecology Letters* 12: 735–743.

Rabosky, D. L. 2010. Extinction rates should not be estimated from molecular phylogenies. *Evolution* 64: 1816–1824.

Rabosky, D. L. 2014. Automatic detection of key innovations, rate shifts, and diversity-dependence on phylogenetic trees. *PLoS One* 9: e89543.

Rada, F. 2016. Functional diversity in tropical high elevation giant rosettes. *In* G. Goldstein, and L. S. Santiago [eds.], Tropical tree physiology: Adaptations and responses in a changing environment, 181–202. Springer International Publishing, New York, NY, USA.

Rada, F., G. Goldstein, A. Azocar, and F. Meinzer. 1985. Freezing avoidance in Andean giant rosette plants. *Plant, Cell & Environment* 8: 501–507.

Revell, L. J. 2012. phytools: An R package for phylogenetic comparative biology (and other things). *Methods in Ecology and Evolution* 3: 217–223.

Roquet, C., F. C. Boucher, W. Thuiller, and S. Lavergne. 2013. Replicated radiations of the alpine genus *Androsace* (Primulaceae) driven by range expansion and convergent key innovations. *Journal of Biogeography* 40: 1874–1886.

Rundell, R. J., and T. D. Price. 2009. Adaptive radiation, nonadaptive radiation, ecological speciation and nonecological speciation. *Trends in Ecology & Evolution* 24: 394–399.

Sanderson, M. J. 2003. r8s: Inferring absolute rates of molecular evolution and divergence times in the absence of a molecular clock. *Bioinformatics* 19: 301–302.

Schluter, D. 2000. The ecology of adaptive radiation. Oxford University Press, Oxford, UK.

Simões, M., L. Breitkreuz, M. Alvarado, S. Baca, J. C. Cooper, L. Heins, K. Herzog, and B. S. Lieberman. 2016. The evolving theory of evolutionary radiations. *Trends in Ecology & Evolution* 31: 27–34.

Simpson, G. G. 1944. Tempo and mode in evolution. Columbia University Press, New York, New York, USA.

Sklenář, P. 1999. Nodding capitula in superpáramo Asteraceae: An adaptation to unpredictable environment. *Biotropica* 31: 394–402.

Sklenář, P., E. Dušková, and H. Balslev. 2011. Tropical and temperate: Evolutionary history of páramo flora. *Botanical Review* 77: 71–108.

Smith, A. P. 1981. Growth and Population Dynamics of *Espeletia* (Compositae) in the Venezuelan Andes. Smithsonian Contributions to Botany, vol. 48. Smithsonian Institution Press, Washington, D.C., USA.

Soulebeau, A., X. Aubriot, M. Gaudeul, G. Rouhan, S. Hennequin, T. Haevermans, J.-Y. Dubuisson, and F. Jabbour. 2015. The hypothesis of adaptive radiation in evolutionary biology: Hard facts about a hazy concept. *Organisms Diversity & Evolution* 15: 747–761.

Stamatakis, A. 2006. RAxML-VI-HPC: Maximum likelihood-based phylogenetic analyses with thousands of taxa and mixed models. *Bioinformatics* 22: 2688–2690.

Testo, W. L., E. Sessa, and D. S. Barrington. 2019. The rise of the Andes promoted rapid diversification in neotropical *Phlegmariurus* (Lycopodiaceae). *New Phytologist* 222: 604–613.

Thuiller, W., S. Lavorel, G. Midgley, S. Lavergne, and T. Rebelo. 2004. Relating plant traits and species distributions along bioclimatic gradients for 88 *Leucadendron* taxa. *Ecology* 85: 1688–1699.

Torres, V., H. Hooghiemstra, L. Lourens, and P. C. Tzedakis. 2013. Astronomical tuning of long pollen records reveals the dynamic history of montane biomes and lake levels in the tropical high Andes during the Quaternary. *Quaternary Science Reviews* 63: 59–72.

Uribe-Convers, S., and D. C. Tank. 2015. Shifts in diversification rates linked to biogeographic movement into new areas: An example of a recent radiation in the Andes. *American Journal of Botany* 102: 1854–1869.

Van der Hammen, T., and A. M. Cleef. 1986. Development of the high Andean paramo flora and vegetation. *In* F. Vuilleumier and M. Monasterio [eds.], High altitude tropical biogeography, 153–201. Oxford University Press, Oxford, UK.

Vargas, O. M., E. M. Ortiz, and B. B. Simpson. 2017. Conflicting phylogenomic signals reveal a pattern of reticulate evolution in a recent high-Andean diversification (Asteraceae: Astereae: *Diplostephium*). *New Phytologist* 214: 1736–1750.

Weir, J. T. 2006. Divergent timing and patterns of species accumulation in lowland and highland neotropical birds. *Evolution* 60: 842–855.

Weir, J. T., and S. Mursleen. 2013. Diversity-dependent cladogenesis and trait evolution in the adaptive radiation of the Auks (aves: Alcidae). *Evolution* 67: 403–416.

Zachos, J. C., G. R. Dickens, and R. E. Zeebe. 2008. An early Cenozoic perspective on greenhouse warming and carbon-cycle dynamics. *Nature* 451: 279–283.

Zhang, J. 2016. spaa: SPecies Association Analysis, version 0.2.2. Website: https://cran.r-project.org/web/packages/spaa/

**TABLE 1**. Environmental and morphological data used to estimate divergence among species. Morphological traits were selected from Mavárez (2019). Here, the growth-form (GF: tree/rosette) refers to the compactness of leaves surrounding the apical meristem (relaxed for trees/compact for rosettes), and to the shape of leaf sheaths (tubular for trees/flat for rosettes).

| | **Environmental** | **Morphological** | |
|---|---|---|---|
| | | **Vegetative** | **Reproductive** |
| Quantitative | Climate (18 bioclimatic variables of WorldClim; Fick and Hijmans, 2017); Elevation; Aspect & Slope (Digital Elevation Model) | Stem Height (SH in cm); Lamina Length (LL, cm); Lamina Width (LW, cm) | Inflorescence Length (IL, cm); Capitulum Diameter (CD, cm); Corolla Length (CL, mm); Flowers Ratio (FLOR, ray/disc flowers); Achene Length (ALM, mm) |
| Discrete | Macro-habitat: Andean Forest (0-absence/1-presence); sub páramo (0-absence/1-presence); proper páramo (0-absence/1-presence); super-páramo (0-absence/1-presence) | Growth Form (GF, 0-tree/1-rosette); Stem Structure (STEM, 0-branched/1-unbranched) | Inflorescence position (IPOS, 0-lateral/1-terminal) |

**FIGURE 1.** A, Map of the northern Andes with the distribution area of *Espeletia*. B, Examples of habitats occupied by *Espeletia*: (1) upper Andean forest; (2) shrubby sub-páramo; (3) open grassland páramo; and (4) rocky super-páramo. C, Examples of morphological diversity in *Espeletia* regarding growth-forms: trees (1. *E. neriifolia*); branched rosettes (2. *E. jahnii*; front);

tall caulescent polycarpic rosettes (2. *E. thyrsiformis*; back, 3. *E. timotensis*); tall caulescent monocarpic rosette (4. *E. figueirasii*); sessile polycarpic rosette (8. *E. nana*); sessile monocarpic rosette (9. *E. jabonensis*); and regarding traits: broad leaves (6. *E. badilloi*) slender leaves (7. *E. vergarae*); lateral inflorescences (3, 8), terminal inflorescences (4, 9), large-size short-ligulate wind-pollinated capitulum (5. *E. moritziana*); medium-size long-ligulate insect-pollinated capitulum (10. *E. schultzii*). Photos by Andreas Gröger (5), Serge Aubert (1-4, 6-10).

**FIGURE 2.** Phylogenetic relationships and divergence times in the Venezuelan clade of *Espeletia*. Node values: left, Bayesian posterior probabilities (BP), right, Maximum-Likelihood bootstrap percentages (ML). Only values smaller than 1.00/100 are shown. Node bars represent 95% confidence intervals for ages. Black star indicates node used for age calibration according to Pouchon et al. (2018). Blue line shows sea surface paleo-temperatures (Zachos et al., 2008). Asterisk (*) represents herbarium sample (MCY 30237).

**FIGURE 3**. Distribution range overlap in the Venezuelan clade of *Espeletia*. A, Niche overlap between species (referred as sympatric rate), estimated according to the Pianka index and the occurrence matrix of species into páramos defined in B. B, Geographic páramo units used for analysis of distribution co-occurrence. C, Mantel correlogram between the distribution overlap distance and the phylogenetic distance. Black boxes are statistically significant ($P < 0.05$), white boxes are not.

**FIGURE 4.** Model selection of lineage diversification according to the delta corrected Akaike Information Criterion comparison (AICc). Models: Pure-Birth (PB), Birth-Death (BD), BD with exponential variation of speciation rate according to time (BDX+T) or paleo-temperatures (BDX+E) (from Zachos et al., 2008), with linear (DDL) or exponential (DDX) rate variation according to diversity-dependence. Models were fitted for 100 dating trees randomly sampled from the posterior distribution in R packages RPANDA (Morlon et al., 2016) and DDD (Etienne et al., 2012).

**FIGURE 5.** Evolution of vegetative (PC1-VEG) and reproductive (PC1-REP) traits in relation with the occupation of habitats (PC1,2-HAB) and/or climatic niches (PC2-CLIM) (PGLS test: * $P < 0.05$; *** $P < 0.001$, see Appendix S3). Contribution of morphological and environmental variables into respective components, and projection of species into these new components are given in Appendices S4–S6. Traits legend: ALM, achene length; CD, capitulum diameter;

FLOR, ray/disc flower ratio; GF.0, non-rosette growth form; IPOS.1, terminal inflorescence; LL, lamina length; LW, lamina width; RFCL, corolla length; SH, stem height; STEM.1, branched stem structure.

**FIGURE 6.** Model selection of trait evolution according to the delta corrected Akaike Information Criterion (dAICc) for vegetative traits (PC1-VEG) and reproductive traits (PC1-REP). Models: BM, Brownian motion; OU, Ornstein-Uhlenbeck; EB, Early-Burst; MC, Matching Competition; and DD, Diversity-Dependent models with linear (DDL) or exponential (DDX) effects. Models were inferred on 100 trees randomly sampled from the posterior distribution. Models were fitted in the R packages "geiger" (Harmon et al., 2008) and "RPANDA" (Morlon et al., 2016).

**FIGURE 7.** Evolutionary trajectories of vegetative (PC1-VEG) and reproductive (PC1-REP) morphotypes through time. Delta values were estimated from model fitted in the R packages "geiger" (Harmon et al., 2008).

Figure 1

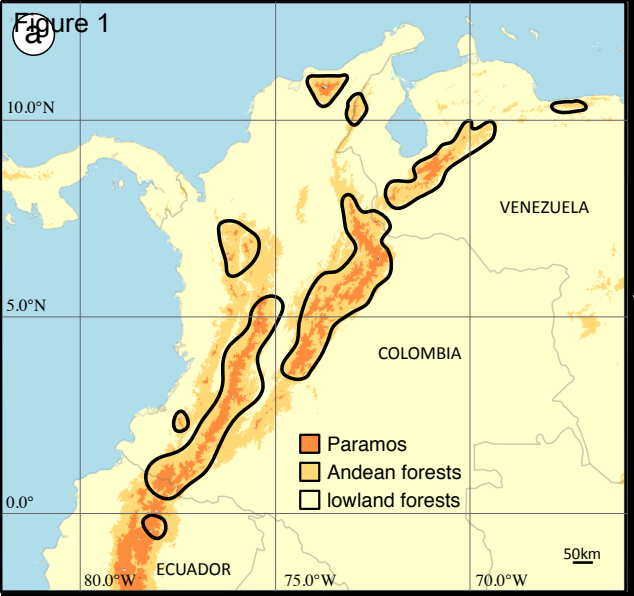




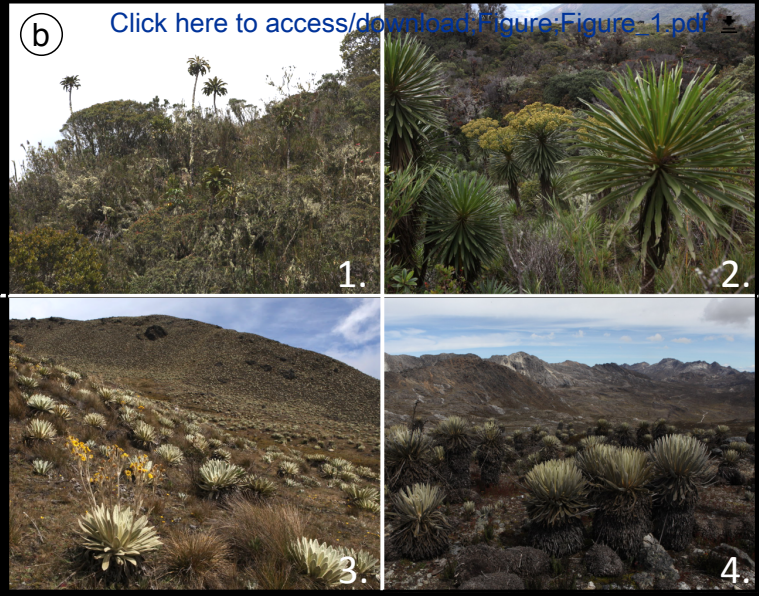


Figure 2



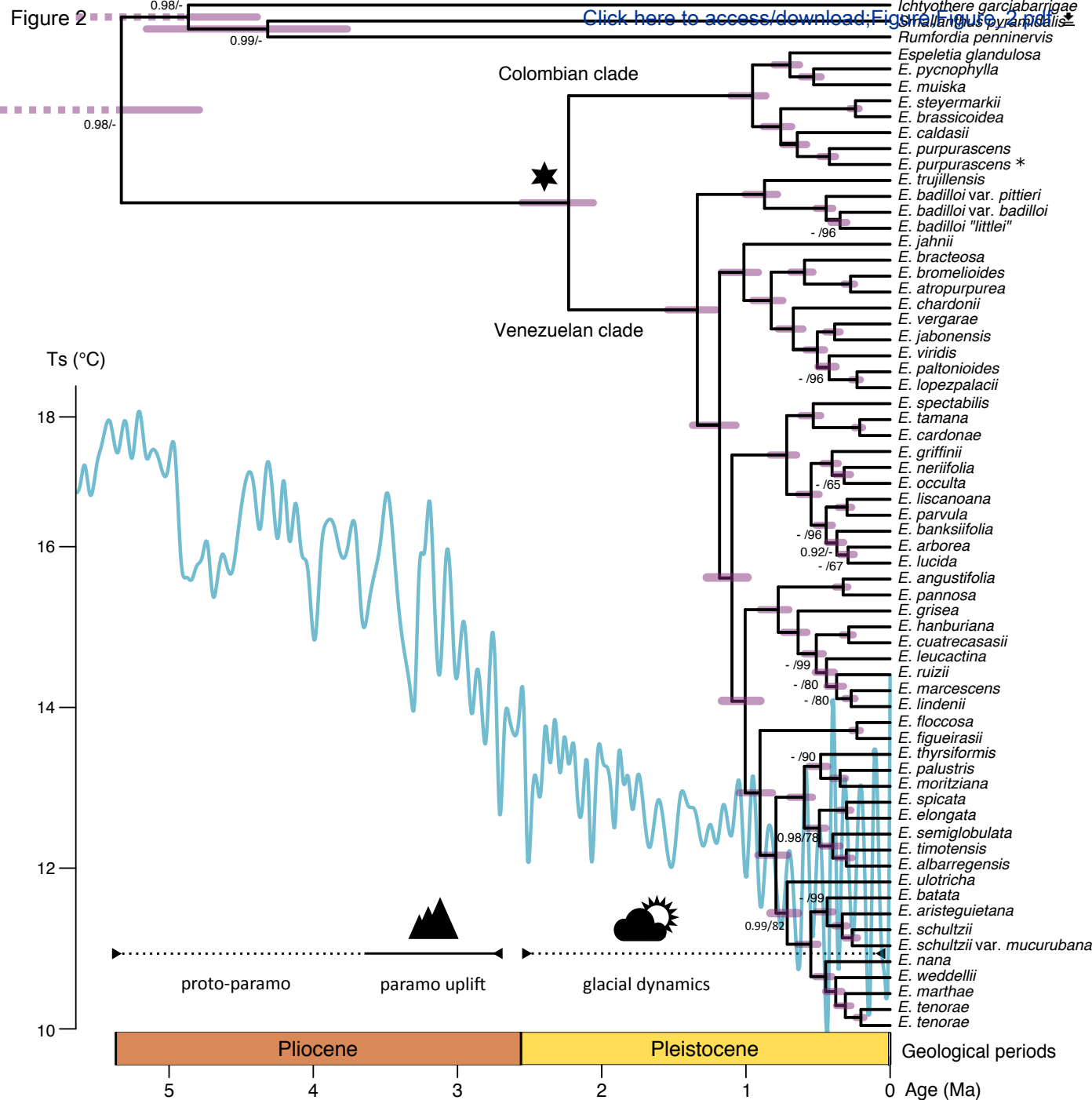

Figure 3



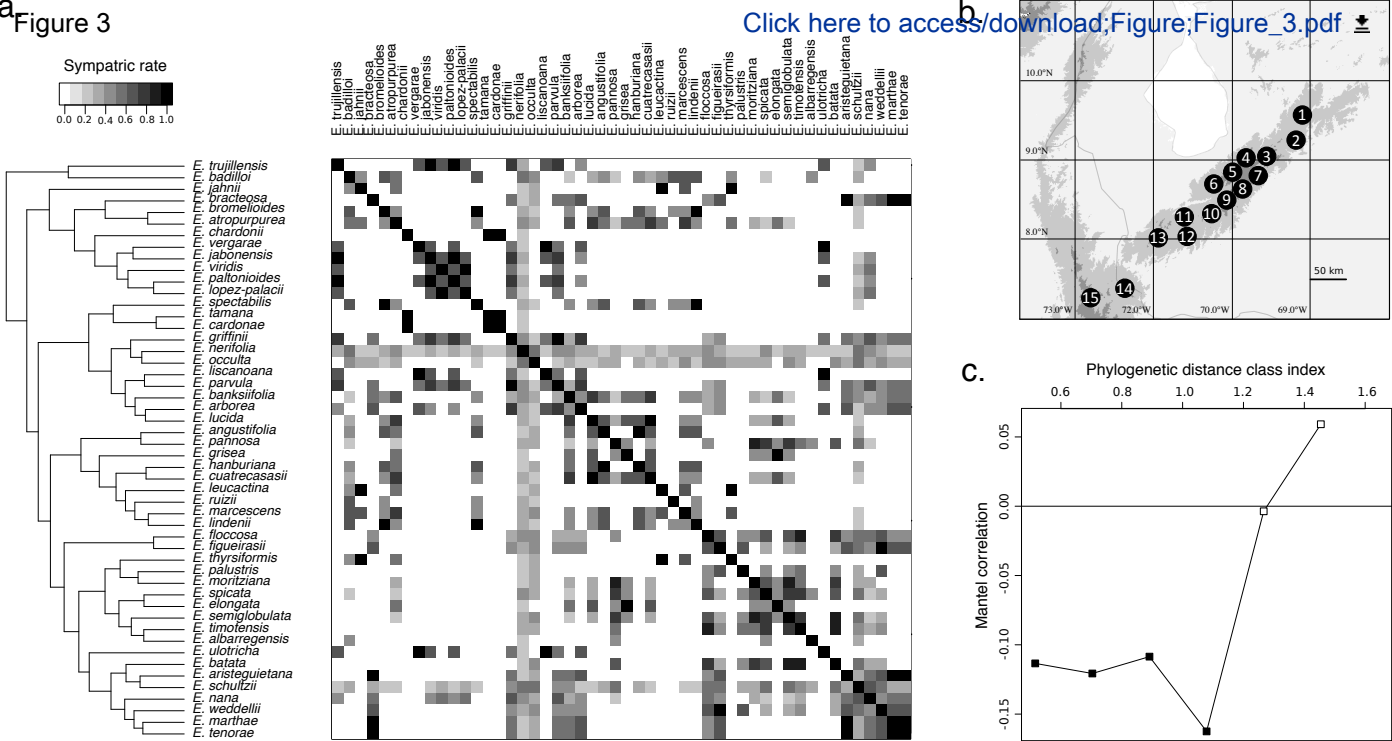

Figure 4

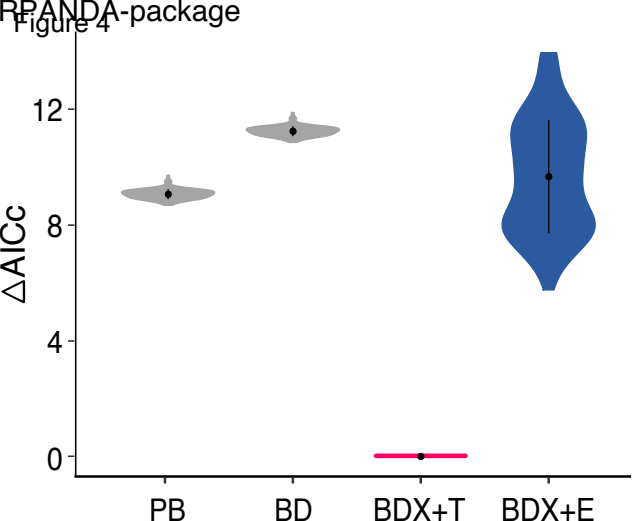
RPANDA-package
ΔAICc
12
8
4
0
PB
BD
BDX+T
BDX+E

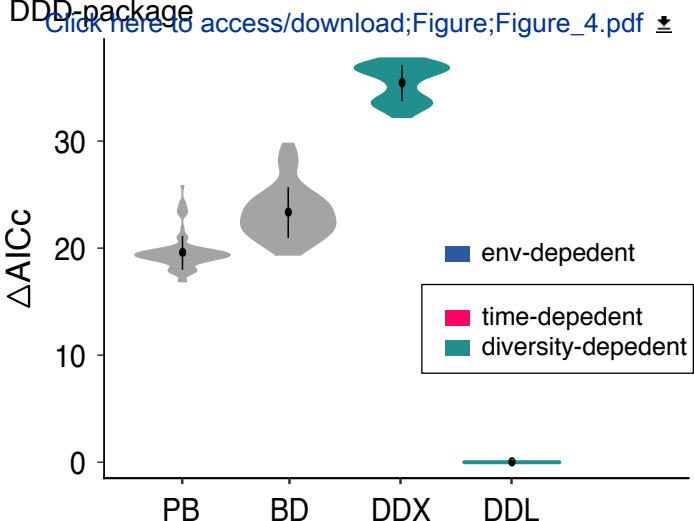
DDD-package
Click here to access/download;Figure;Figure_4.pdf
ΔAICc
30
20
10
0
PB
BD
DDX
DDL
env-depedent
time-depedent
diversity-depedent

Figure 5



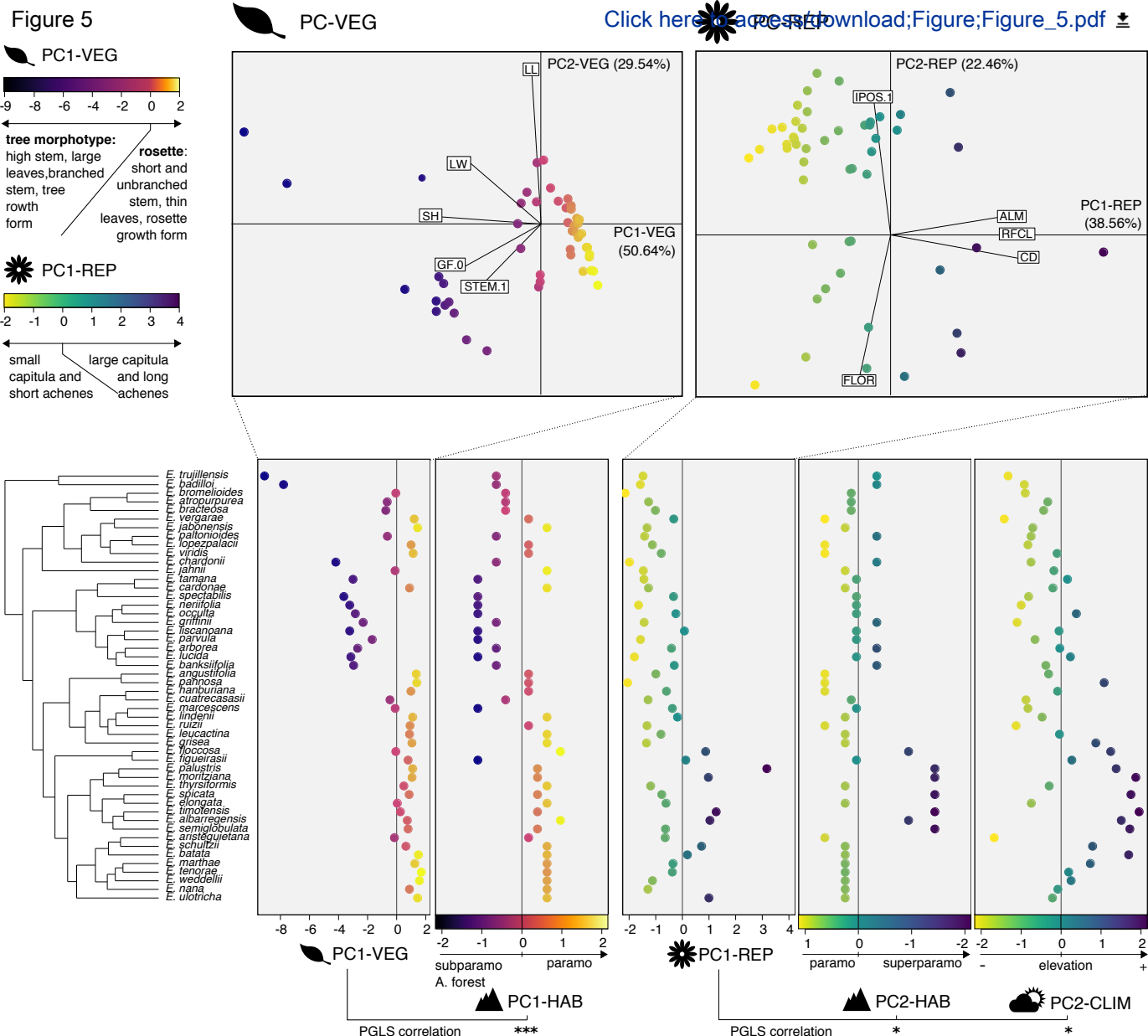

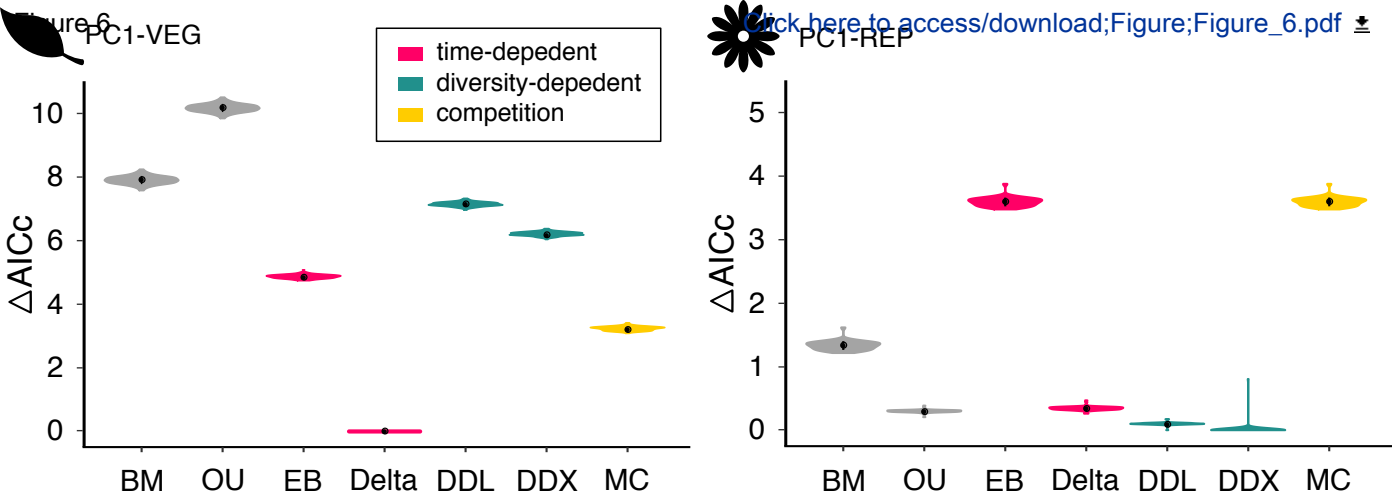

Figure 7

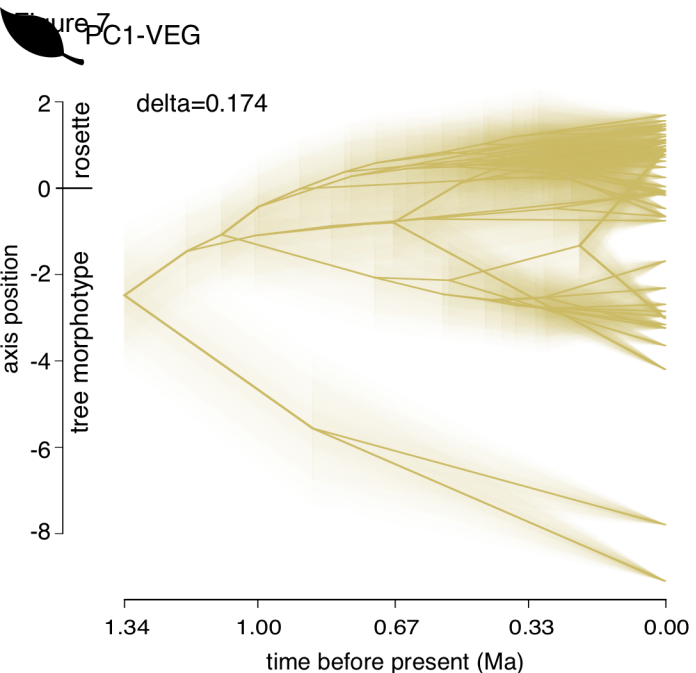


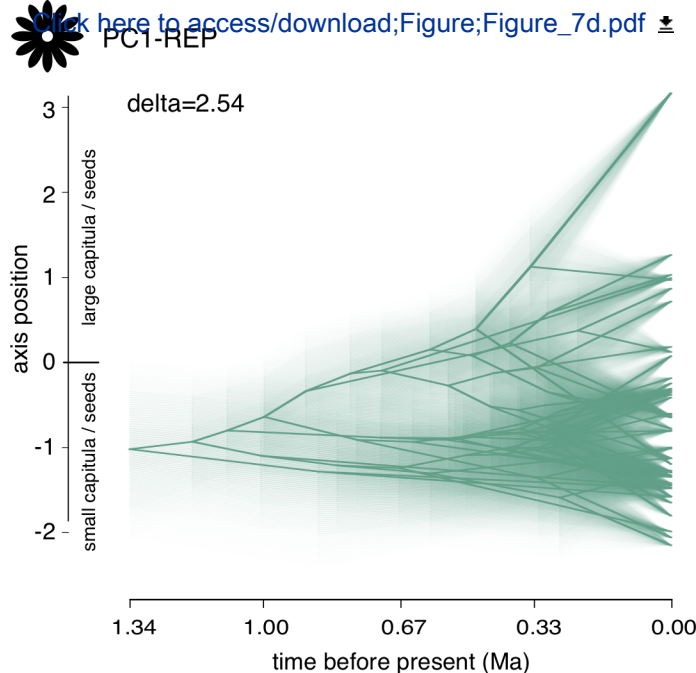

**APPENDIX S1.** Sampling and shotgun libraries preparation.

***Sampling*—**Our sampling now accounts for 16 additional species compared to the most recent phylogeny of the Venezuelan *Espeletia* cade (Pouchon *et al*. 2018). It now includes 92.5% of the 54 recognized species in the clade. Intraspecific samples include three individuals of *E. badilloi* Cuatrec., two of *E. tenorae* Aristeg., two of *E. purpurascens* Cuatrec. ("*" represents sample *López-Figueiras 30237* deposited in herbarium MCY) and two of *E. schultzii* Wedd. We also included *Ichthyothere garciabarrigae* H.Rob. as outgroup according to Diazgranados & Barber (2017), along with *Rumfordia penninervis* S.F.Blake and *Smallanthus pyramidalis* (Triana) H.Rob. Tissue vouchers deposited in collection at Laboratoire d'Ecologie Alpine.

***Shotgun libraries***—Shotgun libraries were prepared and sequenced in an Illumina HiSeq 4000 (2 x150 bp paired-ends) at the Genoscope (Paris, France) or Illumina HiSeq 2000 (2x100 bp paired ends) at Fasteris (Geneva, Switzerland) (see Table S1).

*Genoscope preparation*—A total of 10 ng of genomic DNA were sonicated using the E210 Covaris instrument (Covaris, Inc., USA). Then, fragments were end-repaired, 3'-adenylated and NEXTflex DNA barcoded adapters were added by using NEBNext Ultra II DNA Library prep kit for Illumina (New England Biolabs). After two consecutive 1x AMPure clean ups, the ligated products were PCR-amplified with NEBNext® Ultra II Q5 Master Mix included in the kit, followed by 0.8x AMPure XP purification. All libraries were subjected to size profile analysis conducted by Agilent 2100 Bioanalyzer (Agilent Technologies, USA) and qPCR quantification (MxPro, Agilent Technologies, USA), then sequenced using 151 base-length read chemistry in a paired-end flow cell on the Illumina HiSeq4000 sequencer (Illumina, USA). On average, 15 billion useful paired-end reads were obtained. An Illumina filter was applied to remove the least reliable data from the analysis. The raw data were filtered to remove any clusters with too much intensity corresponding to bases other than the called base. Adapters and primers were removed on the whole read and low quality nucleotides were trimmed from both ends (while quality value is lower than 20). Sequences between the second unknown nucleotide (N) and the end of the read were also removed. Reads shorter than 30 nucleotides after trimming were discarded. Finally, the reads and their mates that mapped onto run quality control sequences (PhiX genome) were removed. These trimming steps were achieved using internal software based on the FastX package (http://hannonlab.cshl.edu/fastx_toolkit/index.html).

| Species | Locality (Country) | Platform | Laboratory | Source |
|---|---|---|---|---|
| *Ichtyothere garciabarrigae* H.Rob. | Colombia | HiSeq 4000 | Genoscope | This paper |
| *Rumfordia penninervis* S.F.Blake. | Mexico | HiSeq 2000 | Fasteris | Pouchon *et al.* (2018) |
| *Smallanthus pyramidalis* (Triana) H.Rob. | Páramo Piedras Blancas (VEN) | HiSeq 2000 | Fasteris | Pouchon *et al.* (2018) |
| *E. albarregensis* (Cuatrec.) Mavárez | Laguna Albarregas (VEN) | HiSeq 4000 | Genoscope | This paper |
| *E. angustifolia* Cuatrec. | Páramo San José (VEN) | HiSeq 2000 | Fasteris | Pouchon *et al.* (2018) |
| *E. arborea* Aristeg. | Laguna Santo Cristo (VEN) | HiSeq 4000 | Genoscope | This paper |
| *E. aristeguietana* Cuatrec. | Páramo La Cristalina (VEN) | HiSeq 2000 | Fasteris | Pouchon *et al.* (2018) |
| *E. atropurpurea* A.C.Sm. | Páramo San José (VEN) | HiSeq 2000 | Fasteris | Pouchon *et al.* (2018) |
| *E. badilloi* var. *badilloi* Cuatrec. | Páramo San José (VEN) | HiSeq 2000 | Fasteris | Pouchon *et al.* (2018) |
| *E. badilloi* « littlei » Cuatrec. | Páramo El Tambor (VEN) | HiSeq 4000 | Genoscope | This paper |
| *E. badilloi* var. *pittieri* (Cuatrec.) Mavárez | Páramo El Molino (VEN) | HiSeq 2000 | Fasteris | Pouchon *et al.* (2018) |

| | | | | |
|---|---|---|---|---|
| *E. banksiifolia* Sch.Bip. & Ettingsh. ex Wedd. | Páramo Los Granates (VEN) | HiSeq 4000 | Genoscope | This paper |
| *E. batata* Cuatrec. | Páramo Piedras Blancas (VEN) | HiSeq 2000 | Fasteris | Pouchon *et al.* (2018) |
| *E. bracteosa* Standl. | Páramo El Arenal (VEN) | HiSeq 2000 | Fasteris | Pouchon *et al.* (2018) |
| *E. brassicoidea* Cuatrec. | Páramo de Tamá (VEN-COL) | HiSeq 2000 | Fasteris | Pouchon *et al.* (2018) |
| *E. bromelioides* Cuatrec. | Páramo El Molino (VEN) | HiSeq 2000 | Fasteris | Pouchon *et al.* (2018) |
| *E. caldasii* Cuatrec. | Páramo Santurbán (COL) | HiSeq 2000 | Fasteris | Pouchon *et al.* (2018) |
| *E. cardonae* Cuatrec. | Páramo de Tamá (VEN-COL) | HiSeq 4000 | Genoscope | This paper |
| *E. chardonii* A.C.Sm. | Páramo de Tamá (VEN-COL) | HiSeq 2000 | Fasteris | Pouchon *et al.* (2018) |
| *E. cuatrecasasii* Ruiz-Terán & López-Fig. | Páramo Don Pedro (VEN) | HiSeq 4000 | Genoscope | This paper |
| *E. elongata* A.C.Sm. | Páramo La Culata (VEN) | HiSeq 4000 | Genoscope | This paper |
| *E. figueirasii* Cuatrec. | Páramo Piedras Blancas (VEN) | HiSeq 2000 | Fasteris | Pouchon *et al.* (2018) |
| *E. floccosa* Standl. | Páramo Piedras Blancas (VEN) | HiSeq 2000 | Fasteris | Pouchon *et al.* (2018) |
| *E. glandulosa* Cuatrec. | Arcabuco (COL) | HiSeq 2000 | Fasteris | Pouchon *et al.* (2018) |
| *E. griffinii* Ruiz-Terán & López-Fig. | Páramo de Guaramacal (VEN) | HiSeq 2000 | Fasteris | Pouchon *et al.* (2018) |
| *E. grisea* Standl. | Páramo Los Nevados (VEN) | HiSeq 4000 | Genoscope | This paper |
| *E. hanburiana* Cuatrec. | Laguna Las Lajas (VEN) | HiSeq 4000 | Genoscope | This paper |
| *E. jabonensis* Cuatrec. | Páramo de Guaramacal (VEN) | HiSeq 2000 | Fasteris | Pouchon *et al.* (2018) |
| *E. jahnii* Standl. | Páramo El Batallón (VEN) | HiSeq 2000 | Fasteris | Pouchon *et al.* (2018) |
| *E. leucactina* Cuatrec. | Páramo El Batallón (VEN) | HiSeq 2000 | Fasteris | Pouchon *et al.* (2018) |
| *E. lindenii* Sch.Bip. ex Wedd. | Páramo San José (VEN) | HiSeq 2000 | Fasteris | Pouchon *et al.* (2018) |
| *E. liscanoana* Cuatrec. | Páramo de Cendé (VEN) | HiSeq 4000 | Genoscope | This paper |
| *E. lopezpalacii* Ruiz-Terán & López-Fig. | Páramo de Guaramacal (VEN) | HiSeq 2000 | Fasteris | Pouchon *et al.* (2018) |
| *E. lucida* Aristeg. | Estación La Aguada (VEN) | HiSeq 4000 | Genoscope | This paper |
| *E. marcescens* S.F.Blake | Páramo San José (VEN) | HiSeq 2000 | Fasteris | Pouchon *et al.* (2018) |
| *E. marthae* Cuatrec. | Páramo Guirigay (VEN) | HiSeq 4000 | Genoscope | This paper |
| *E. moritziana* Sch.Bip. & Ettingsh. ex Wedd. | Páramo Piedras Blancas (VEN) | HiSeq 2000 | Fasteris | Pouchon *et al.* (2018) |
| *E. muiska* Cuatrec. | Arcabuco (COL) | HiSeq 4000 | Genoscope | This paper |
| *E. nana* Cuatrec. | Páramo El Arenal (VEN) | HiSeq 2000 | Fasteris | Pouchon *et al.* (2018) |
| *E. neriifolia* (Bonpl. ex Humb.) Sch.Bip. ex Wedd. | Páramo El Arenal (VEN) | HiSeq 2000 | Fasteris | Pouchon *et al.* (2018) |
| *E. occulta* S.F.Blake | Páramo Piedras Blancas (VEN) | HiSeq 2000 | Fasteris | Pouchon *et al.* (2018) |
| *E. paltonioides* Standl. | Páramo de Guaramacal (VEN) | HiSeq 2000 | Fasteris | Pouchon *et al.* (2018) |
| *E. palustris*(Diazgr. & Morillo) Mavárez | Páramo Piedras Blancas (VEN) | HiSeq 2000 | Fasteris | Pouchon *et al.* (2018) |
| *E. pannosa* Standl. | Páramo Los Nevados (VEN) | HiSeq 2000 | Fasteris | Pouchon *et al.* (2018) |
| *E. parvula* (Cuatrec.) Mavárez | Páramo de Cendé (VEN) | HiSeq 4000 | Genoscope | This paper |
| *E. purpurascens* Cuatrec. | Páramo de Tamá (VEN-COL) | HiSeq 2000 | Fasteris | Pouchon *et al.* (2018) |
| **E. purpurascens* Cuatrec. | Páramo de Tamá (VEN-COL) | HiSeq 2000 | Fasteris | This paper |
| *E. pycnophylla* Cuatrec. | Páramo El Angel (Ecuador) | HiSeq 4000 | Genoscope | This paper |
| *E. ruizii* Cuatrec. | Páramo El Molino (VEN) | HiSeq 2000 | Fasteris | Pouchon *et al.* (2018) |
| *E. schultzii* var. *schultzii* Wedd. | Páramo Piedras Blancas (VEN) | HiSeq 2000 | Fasteris | Pouchon *et al.* (2018) |
| *E. schultzii* var. *mucurubana* Cuatrec. | Páramo Piedras Blancas (VEN) | HiSeq 2000 | Fasteris | Pouchon *et al.* (2018) |
| *E. spicata* Cuatrec. | Páramo Piedras Blancas (VEN) | HiSeq 2000 | Fasteris | Pouchon *et al.* (2018) |
| *E. semiglobulata* Cuatrec. | Páramo Piedras Blancas (VEN) | HiSeq 2000 | Fasteris | Pouchon *et al.* (2018) |
| *E. steyermarkii* Cuatrec. | Páramo de Tamá (VEN-COL) | HiSeq 2000 | Fasteris | Pouchon *et al.* (2018) |
| *E. spectabilis* Cuatrec. | Páramo San José (VEN) | HiSeq 2000 | Fasteris | Pouchon *et al.* (2018) |
| *E. tamana* Cuatrec. | Páramo de Tamá (VEN-COL) | HiSeq 4000 | Genoscope | This paper |
| *E. tenorae* Aristeg. | Páramo Guirigay (VEN) | HiSeq 2000 | Fasteris | This paper |
| *E. tenorae* Aristeg. | Páramo Guirigay (VEN) | HiSeq 4000 | Genoscope | This paper |
| *E. thyrsiformis* A.C.Sm. | Páramo El Batallón (VEN) | HiSeq 2000 | Fasteris | Pouchon *et al.* (2018) |
| *E. timotensis* Cuatrec. | Páramo Piedras Blancas (VEN) | HiSeq 2000 | Fasteris | Pouchon *et al.* (2018) |

| | | | | |
|---|---|---|---|---|
| *E. trujillensis* Cuatrec. | Páramo de Guaramacal (VEN) | HiSeq 2000 | Fasteris | Pouchon *et al.* (2018) |
| *E. ulotricha* Cuatrec. | Páramo Cendé (VEN) | HiSeq 4000 | Genoscope | This paper |
| *E. vergarae* (Cuatrec. & López-Fig.) Mavárez | Páramo Cendé (VEN) | HiSeq 2000 | Fasteris | Pouchon *et al.* (2018) |
| *E. viridis* Aristeg. | Páramo de Guaramacal (VEN) | HiSeq 2000 | Fasteris | Pouchon *et al.* (2018) |
| *E. weddellii* Sch.Bip. ex Wedd. | Páramo Guirigay (VEN) | HiSeq 4000 | Genoscope | This paper |

**Literature cited:**

Diazgranados, M. & Barber, J.C. (2017). Geography shapes the phylogeny of frailejones (Espeletiinae Cuatrec., Asteraceae): a remarkable example of recent rapid radiation in sky islands. *PeerJ*, 5.

Pouchon, C., Fernández, A., Nassar, J.M., Boyer, F., Aubert, S., Lavergne, S., *et al*. (2018). Phylogenomic Analysis of the Explosive Adaptive Radiation of the Espeletia Complex (Asteraceae) in the Tropical Andes. *Systematic Biology*, 67, 1041–1060.

**APPENDIX S2a.** Bioinformatic pipeline of nuclear genomic regions reconstructions. A total of 9880 nuclear metacontigs were assembled in Pouchon et al. (2018) from species contigs assemblies (panel a.)**.** The metacontigs were used as a reference database to align the sequencing reads of samples from Pouchon et al. (2018) and this paper (panel b). PNR: potential nuclear reads, defined in Pouchon et al. (2018).

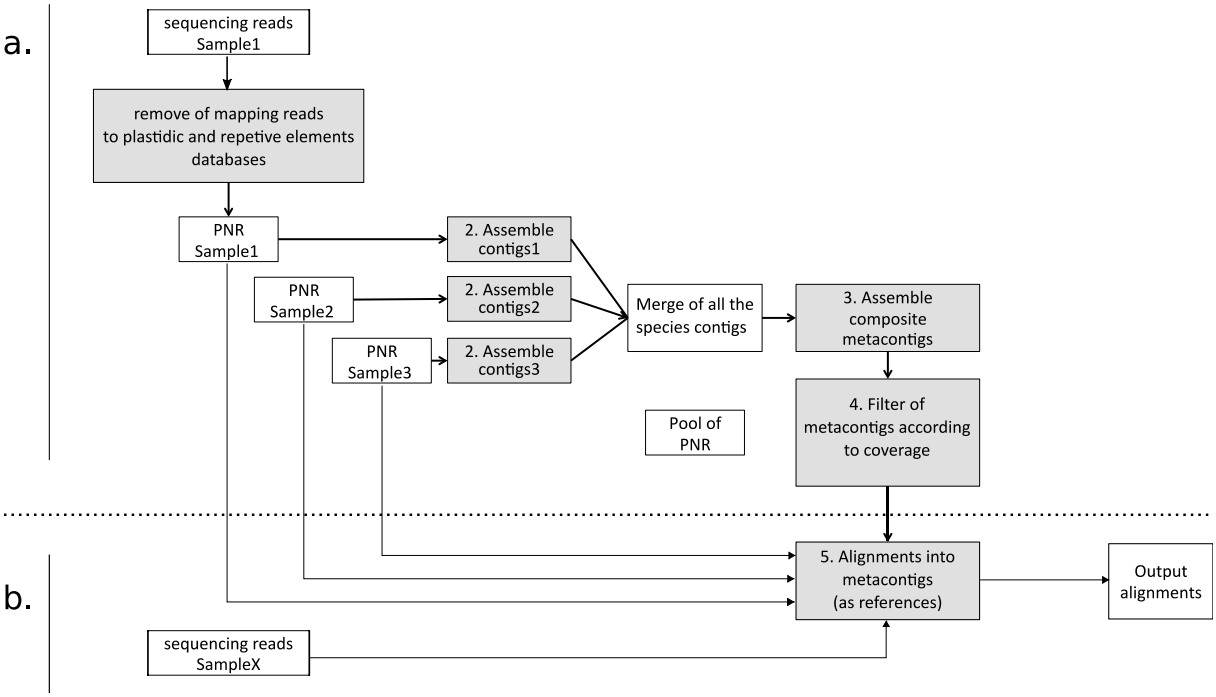


**APPENDIX S2b.** Summary statistics over sequencing and phylogenetic alignments.

| Species | # Reads | # Consensus alignments (/9880 metacontigs) | % Missing data in concatenated alignment |
|---|---|---|---|
| *Ichtyothere garciabarrigae* | 12502596 | 421 | 0.97 |
| *Rumfordia penninervis* | 17321123 | 291 | 0.98 |
| *Smallanthus pyramidalis* | 15267267 | 204 | 0.98 |
| *E. albarregensis* | 13624268 | 6814 | 0.4 |
| *E. angustifolia* | 16507894 | 7507 | 0.33 |
| *E. arborea* | 19375927 | 6924 | 0.38 |
| *E. aristeguietana* | 10939974 | 6857 | 0.4 |
| *E. atropurpurea* | 17430030 | 6813 | 0.4 |
| *E. badilloi* var. *badilloi* | 4984893 | 5015 | 0.58 |
| *E. badilloi* « *littlei* » | 13967599 | 5842 | 0.49 |
| *E. badilloi* var. *pittieri* | 16054991 | 6274 | 0.46 |
| *E. banksiifolia* | 13914324 | 6817 | 0.4 |
| *E. batata* | 7925776 | 6708 | 0.43 |
| *E. bracteosa* | 8684341 | 6340 | 0.45 |
| *E. brassicoidea* | 7201499 | 4925 | 0.55 |
| *E. bromelioides* | 18849924 | 6772 | 0.4 |
| *E. caldasii* | 15045803 | 4650 | 0.57 |

| | | | |
|---|---|---|---|
| *E. cardonae* | 17611496 | 6907 | 0.36 |
| *E. chardonii* | 19319750 | 6514 | 0.42 |
| *E. cuatrecasasii* | 16068464 | 7016 | 0.37 |
| *E. elongata* | 15888163 | 6919 | 0.38 |
| *E. figueirasii* | 20081214 | 6705 | 0.42 |
| *E. floccosa* | 6297993 | 5926 | 0.51 |
| *E. glandulosa* | 18501072 | 5004 | 0.54 |
| *E. griffinii* | 4231602 | 5739 | 0.53 |
| *E. grisea* | 14185999 | 6917 | 0.38 |
| *E. hanburiana* | 13880023 | 6901 | 0.39 |
| *E. jabonensis* | 12855749 | 6386 | 0.44 |
| *E. jahnii* | 18753847 | 6199 | 0.47 |
| *E. leucactina* | 11290989 | 6697 | 0.42 |
| *E. lindenii* | 6845497 | 6619 | 0.43 |
| *E. liscanoana* | 13745751 | 6534 | 0.42 |
| *E. lopezpalacii* | 7247985 | 5794 | 0.51 |
| *E. lucida* | 14565009 | 6997 | 0.37 |
| *E. marcescens* | 4966632 | 6478 | 0.45 |
| *E. marthae* | 17955204 | 7023 | 0.37 |
| *E. moritziana* | 8136454 | 6382 | 0.46 |
| *E. muiska* | 17979510 | 5303 | 0.52 |
| *E. nana* | 8224828 | 6804 | 0.41 |
| *E. neriifolia* | 10670853 | 6632 | 0.43 |
| *E. occulta* | 5535336 | 6095 | 0.49 |
| *E. paltonioides* | 20985038 | 6559 | 0.42 |
| *E. palustris* | 13521468 | 7192 | 0.37 |
| *E. pannosa* | 14077121 | 7384 | 0.35 |
| *E. parvula* | 18564613 | 7016 | 0.36 |
| *E. purpurascens* | 4237288 | 4565 | 0.59 |
| *E. purpurascens* * | 1035670 | 3392 | 0.73 |
| *E. pycnophylla* | 12541626 | 4736 | 0.58 |
| *E. ruizii* | 16367539 | 7048 | 0.38 |
| *E. schultzii* var. *schultzii* | 11155891 | 7062 | 0.38 |
| *E. schultzii* var. *mucurubana* | 10477041 | 7066 | 0.39 |
| *E. spicata* | 35903204 | 7205 | 0.36 |
| *E. semiglobulata* | 6202382 | 5932 | 0.51 |
| *E. steyermarkii* | 11429995 | 5278 | 0.52 |
| *E. spectabilis* | 7060812 | 6742 | 0.4 |
| *E. tamana* | 15436060 | 6799 | 0.38 |
| *E. tenorae* 1 | 2550565 | 5443 | 0.56 |
| *E. tenorae* 2 | 17243779 | 6766 | 0.4 |
| *E. thyrsiformis* | 8117807 | 6629 | 0.44 |
| *E. timotensis* | 22914069 | 6925 | 0.39 |
| *E. trujillensis* | 8127220 | 5296 | 0.55 |
| *E. ulotricha* | 13284214 | 6296 | 0.45 |
| *E. vergarae* | 14247110 | 6569 | 0.43 |
| *E. viridis* | 25079044 | 6883 | 0.39 |
| *E. weddellii* | 18666964 | 7556 | 0.29 |

**Literature cited:**

Pouchon, C., Fernández, A., Nassar, J.M., Boyer, F., Aubert, S., Lavergne, S., *et al*. (2018). Phylogenomic Analysis of the Explosive Adaptive Radiation of the Espeletia Complex (Asteraceae) in the Tropical Andes. *Systematic Biology*, 67, 1041–1060.

**APPENDIX S3.** Table summarizing the distribution of species into the main páramo units.

Distribution of *Espeletia* into the 15 main páramo units given in the Fig. 3b, adapted from Mavárez (2019). Note: 0-absence; 1-presence. Localities: (1) Páramo del Jabón, (2) Páramo Guaramacal, (3) Las Mesitas/Jajó/La Morita, (4) Pico el Aguila, (5) Páramo Piedras Blancas, (6) Laguna Albarregas, (7) Laguna Negra, (8) Páramo de Gavidia, (9) La Mucuy/La Aguada, (10) Páramo de San Jose, (11) Páramo el Tambor, (12) Páramo Las Coloradas, (13) Páramo Batallon/La Negra, (14) Páramo de Tama, (15) Páramo de Fontibón.

| Species | 1 | 2 | 3 | 4 | 5 | 6 | 7 | 8 | 9 | 10 | 11 | 12 | 13 | 14 | 15 |
|---|---|---|---|---|---|---|---|---|---|---|---|---|---|---|---|
| *E. albarregensis* | 0 | 0 | 0 | 0 | 0 | 1 | 0 | 0 | 0 | 0 | 0 | 0 | 0 | 0 | 0 |
| *E. angustifolia* | 0 | 0 | 0 | 0 | 0 | 0 | 0 | 0 | 0 | 1 | 0 | 0 | 0 | 0 | 0 |
| *E. arborea* | 1 | 0 | 1 | 0 | 0 | 0 | 0 | 0 | 0 | 0 | 0 | 0 | 0 | 0 | 0 |
| *E. aristeguietana* | 0 | 0 | 1 | 0 | 0 | 0 | 0 | 0 | 0 | 0 | 0 | 0 | 0 | 0 | 0 |
| *E. atropurpurea* | 0 | 0 | 0 | 0 | 0 | 0 | 0 | 0 | 1 | 1 | 0 | 0 | 1 | 0 | 0 |
| *E. badilloi* | 0 | 0 | 0 | 0 | 0 | 1 | 0 | 0 | 0 | 1 | 1 | 1 | 1 | 0 | 0 |
| *E. banksiifolia* | 0 | 0 | 1 | 0 | 0 | 0 | 0 | 0 | 1 | 1 | 0 | 0 | 0 | 0 | 0 |
| *E. batata* | 0 | 0 | 0 | 1 | 1 | 0 | 1 | 1 | 0 | 0 | 0 | 0 | 0 | 0 | 0 |
| *E. bracteosa* | 0 | 0 | 1 | 0 | 0 | 0 | 0 | 0 | 0 | 0 | 0 | 0 | 0 | 0 | 0 |
| *E. bromelioides* | 0 | 0 | 0 | 0 | 0 | 0 | 0 | 0 | 0 | 1 | 1 | 0 | 0 | 0 | 0 |
| *E. cardonae* | 0 | 0 | 0 | 0 | 0 | 0 | 0 | 0 | 0 | 0 | 0 | 0 | 0 | 1 | 0 |
| *E. chardonii* | 0 | 0 | 0 | 0 | 0 | 0 | 0 | 0 | 0 | 0 | 0 | 0 | 0 | 1 | 0 |
| *E. cuatrecasasii* | 0 | 0 | 0 | 0 | 0 | 0 | 0 | 0 | 0 | 1 | 1 | 0 | 0 | 0 | 0 |
| *E. elongata* | 0 | 0 | 0 | 0 | 0 | 0 | 0 | 0 | 1 | 0 | 0 | 0 | 0 | 0 | 0 |
| *E. figueirasii* | 0 | 0 | 1 | 0 | 0 | 0 | 1 | 0 | 0 | 0 | 0 | 0 | 0 | 0 | 0 |
| *E. floccosa* | 0 | 0 | 1 | 1 | 1 | 0 | 1 | 0 | 0 | 0 | 0 | 0 | 0 | 0 | 0 |
| *E. griffinii* | 1 | 1 | 1 | 0 | 0 | 0 | 0 | 0 | 0 | 0 | 0 | 0 | 0 | 0 | 0 |
| *E. grisea* | 0 | 0 | 0 | 0 | 0 | 0 | 0 | 0 | 1 | 0 | 0 | 0 | 0 | 0 | 0 |
| *E. hanburiana* | 0 | 0 | 0 | 0 | 0 | 0 | 0 | 0 | 0 | 1 | 0 | 0 | 0 | 0 | 0 |

| | | | | | | | | | | | | | | | |
|---|---|---|---|---|---|---|---|---|---|---|---|---|---|---|---|
| *E. jabonensis* | 1 | 1 | 0 | 0 | 0 | 0 | 0 | 0 | 0 | 0 | 0 | 0 | 0 | 0 | 0 |
| *E. jahnii* | 0 | 0 | 0 | 0 | 0 | 0 | 0 | 0 | 0 | 0 | 0 | 0 | 1 | 0 | 0 |
| *E. leucactina* | 0 | 0 | 0 | 0 | 0 | 0 | 0 | 0 | 0 | 0 | 0 | 0 | 1 | 0 | 0 |
| *E. lindenii* | 0 | 0 | 0 | 0 | 0 | 0 | 0 | 0 | 0 | 1 | 1 | 0 | 0 | 0 | 0 |
| *E. liscanoana* | 1 | 0 | 0 | 0 | 0 | 0 | 0 | 0 | 0 | 0 | 0 | 0 | 0 | 0 | 0 |
| *E. lopezpalacii* | 0 | 1 | 0 | 0 | 0 | 0 | 0 | 0 | 0 | 0 | 0 | 0 | 0 | 0 | 0 |
| *E. lucida* | 0 | 0 | 0 | 0 | 0 | 0 | 0 | 0 | 1 | 1 | 0 | 0 | 0 | 0 | 0 |
| *E. marcescens* | 0 | 0 | 0 | 0 | 0 | 0 | 0 | 0 | 0 | 1 | 0 | 0 | 1 | 0 | 0 |
| *E. marthae* | 0 | 0 | 1 | 0 | 0 | 0 | 0 | 0 | 0 | 0 | 0 | 0 | 0 | 0 | 0 |
| *E. moritziana* | 0 | 0 | 0 | 1 | 1 | 0 | 0 | 1 | 1 | 0 | 0 | 0 | 0 | 0 | 0 |
| *E. nana* | 0 | 1 | 1 | 1 | 0 | 0 | 0 | 0 | 0 | 0 | 0 | 0 | 0 | 0 | 0 |
| *E. neriifolia* | 1 | 1 | 1 | 1 | 0 | 1 | 1 | 0 | 1 | 1 | 1 | 1 | 1 | 1 | 1 |
| *E. occulta* | 0 | 0 | 1 | 1 | 0 | 0 | 1 | 1 | 0 | 1 | 0 | 1 | 1 | 0 | 0 |
| *E. paltonioides* | 1 | 1 | 0 | 0 | 0 | 0 | 0 | 0 | 0 | 0 | 0 | 0 | 0 | 0 | 0 |
| *E. palustris* | 0 | 0 | 0 | 0 | 0 | 0 | 1 | 0 | 0 | 0 | 0 | 0 | 0 | 0 | 0 |
| *E. pannosa* | 0 | 0 | 0 | 1 | 1 | 1 | 0 | 1 | 1 | 0 | 0 | 0 | 0 | 0 | 0 |
| *E. parvula* | 1 | 1 | 1 | 0 | 0 | 0 | 0 | 0 | 0 | 0 | 0 | 0 | 0 | 0 | 0 |
| *E. ruizii* | 0 | 0 | 0 | 0 | 0 | 0 | 0 | 0 | 0 | 0 | 0 | 1 | 1 | 0 | 0 |
| *E. schultzii* | 0 | 1 | 1 | 1 | 0 | 1 | 1 | 1 | 0 | 1 | 0 | 0 | 0 | 0 | 0 |
| *E. spicata* | 0 | 0 | 0 | 1 | 1 | 1 | 1 | 0 | 1 | 0 | 0 | 0 | 0 | 0 | 0 |
| *E. semiglobulata* | 0 | 0 | 0 | 1 | 1 | 0 | 1 | 1 | 1 | 0 | 0 | 0 | 0 | 0 | 0 |
| *E. spectabilis* | 0 | 0 | 0 | 0 | 0 | 0 | 0 | 0 | 0 | 1 | 1 | 0 | 0 | 0 | 0 |
| *E. tamana* | 0 | 0 | 0 | 0 | 0 | 0 | 0 | 0 | 0 | 0 | 0 | 0 | 0 | 1 | 0 |
| *E. tenorae* | 0 | 0 | 1 | 0 | 0 | 0 | 0 | 0 | 0 | 0 | 0 | 0 | 0 | 0 | 0 |
| *E. thyrsiformis* | 0 | 0 | 0 | 0 | 0 | 0 | 0 | 0 | 0 | 0 | 0 | 0 | 1 | 0 | 0 |

| | | | | | | | | | | | | | | | |
|---|---|---|---|---|---|---|---|---|---|---|---|---|---|---|---|
| *E. timotensis* | 0 | 0 | 0 | 1 | 1 | 0 | 1 | 0 | 0 | 0 | 0 | 0 | 0 | 0 | 0 |
| *E. trujillensis* | 1 | 1 | 0 | 0 | 0 | 0 | 0 | 0 | 0 | 0 | 0 | 0 | 0 | 0 | 0 |
| *E. ulotricha* | 1 | 0 | 0 | 0 | 0 | 0 | 0 | 0 | 0 | 0 | 0 | 0 | 0 | 0 | 0 |
| *E. vergarae* | 1 | 0 | 0 | 0 | 0 | 0 | 0 | 0 | 0 | 0 | 0 | 0 | 0 | 0 | 0 |
| *E. viridis* | 0 | 1 | 0 | 0 | 0 | 0 | 0 | 0 | 0 | 0 | 0 | 0 | 0 | 0 | 0 |
| *E. weddellii* | 0 | 0 | 1 | 0 | 0 | 0 | 1 | 0 | 0 | 0 | 0 | 0 | 0 | 0 | 0 |

**Literature cited:**

Mavárez, J. 2019. A Taxonomic Revision of *Espeletia* (Asteraceae). The Venezuelan Radiation. *Harvard papers in botany* 24: 114.

**APPENDIX S4.** Estimation of speciation rates through time under BAMM model.

Variation of speciation rates through time of lineages was estimated using BAMM (Rabosky 2014) in addition to RPANDA models (Morlon *et al*. 2016). We ran analyses with four reversible jump MCMC chains, each with 10 million of generations and sampled every 10,000 generations for the 200 Bayesian chronograms. Value of the Poisson process rate prior was set to 1.0 to minimize the number of shifts under the prior alone. Priors for both speciation and extinction rates was determined using the setBAMMpriors function, of the 'BAMMtools' R package v.2.1.7 (Rabosky *et al*. 2014). After a burn-in of 10%, MCMC stationarity and (ESS) were assessed in R using the package CODA v.0.19-2 (Plummer *et al*. 2006). BAMM outputs were analysed into 'BAMMtools' to plot the estimated speciation rates through times (phylorate).

**Literature cited:**

Morlon, H., E. Lewitus, F. L. Condamine, M. Manceau, J. Clavel, and J. Drury. 2016. RPANDA: an R package for macroevolutionary analyses on phylogenetic trees. *Methods in Ecology and Evolution* 7: 589–597.

Plummer, M., Best, N., Cowles, K. & Vines, K. (2006). CODA: convergence diagnosis and output analysis for MCMC. *R News*, 6, 7–11.

Rabosky, D.L., Grundler, M., Anderson, C., Title, P., Shi, J.J., Brown, J.W., *et al*. (2014). BAMMtools: an R package for the analysis of evolutionary dynamics on phylogenetic trees. *Methods in Ecology and Evolution*, 5, 701–707.

**APPENDIX S5.** Comparison of geographic range overlap between sister and non-sister species.

Comparison of geographic range overlap between sister and non-sister species. Overlap was estimated according to the Pianka index (in 'spaa' R-package, Zhang, 2016) from the distribution of species into the 15 main units of páramos (see Table S2, Fig. 3b). Sister-species appeared to be significantly more sympatric than non-sister taxa (Kruskall-Wallis test: chi-square = 16.464; df=1; P less than 0.001).

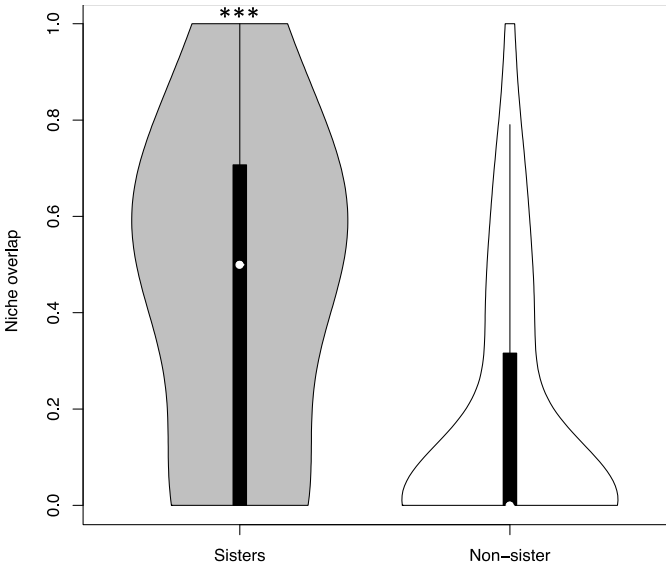


**Literature cited:**

Zhang, J. (2016). *spaa: SPecies Association Analysis*.

**APPENDIX S6.** Table summarizing the estimates of lineages diversification model.

Fitted models of lineage diversification explored for the consensus dating tree. Models: Pure-Birth (PB), Birth-Death (BD), BD with linear exponential (BDX+T) variation of speciation rate according to time, with exponential variation of speciation rate according to paleo-tempartures (BDX+E, from Zachos *et al*., 2008), with linear (DDL) or exponential (DDX) rate variation with diversity-dependence. Time and diversity dependent models are expected in scenario of ecological divergence. Note: Lambda-speciation rate; mu-extinction rate; Loglik-log likelihood; AICc- corrected Akaike Information Criterion; dAICc-delta AICc. Time-dependent and Environmental-dependent models were fitted in 'RPANDA' (Morlon et al., 2016) whereas diversity-dependent models were fitted in the R package 'DDD' (Etienne et al., 2012).

| Models | | Lambda | mu | params | Loglik | AICc | dAICc |
|---|---|---|---|---|---|---|---|
| | PB | 1.835 | 0.000 | - | -20.699 | 43.481 | 8.948 |
| | BD | 1.835 | 2.9e-9 | - | -20.699 | 45.653 | 11.120 |
| Time effect | **BDX+T** | 0.9237 | 3.2e-8 | α=1.604 | -14.005 | 34.533 | 0 |
| Env effect | BDX+E | 0.2501 | 3.9e-4 | α=0.161 | -19.101 | 44.725 | 10.192 |
| | PB | 1.973 | 0 .000 | - | -17.641 | 36.338 | 19.138 |
| | BD | 1.921 | 0.065 | - | - 16.860 | 37.981 | 20.781 |
| Diversity effect | **DDL** | 5.724 | 1.4e-4 | K=56.358 | -6.5039 | 17.200 | **0** |
| | DDX | 9.515 | 2.341 | K=196.68 | -17.856 | 42.246 | 25.046 |

**Literature cited:**

Etienne, R. S., H. Morlon, and A. Lambert. 2012. Estimating the Duration of Speciation from Phylogenies. *Evolution* 68: 2430–2440.

Morlon, H., E. Lewitus, F. L. Condamine, M. Manceau, J. Clavel, and J. Drury. 2016. RPANDA: an R package for macroevolutionary analyses on phylogenetic trees. *Methods in Ecology and Evolution* 7: 589–597.

Zachos, J.C., Dickens, G.R. & Zeebe, R.E. (2008). An early Cenozoic perspective on greenhouse warming and carbon-cycle dynamics. *Nature*, 451, 279–283.

**APPENDIX S7.** Variation of speciation rate through time in the Venezuelan clade of *Espeletia*.

Slowdown in speciation rate to present under models with exponential variation of speciation rate through time and constant extinction rate, estimated in both 'BAMM' (Rabosky 2014) and 'RPANDA' (Morlon et al., 2016) (i.e PBX+T model in RPANDA).

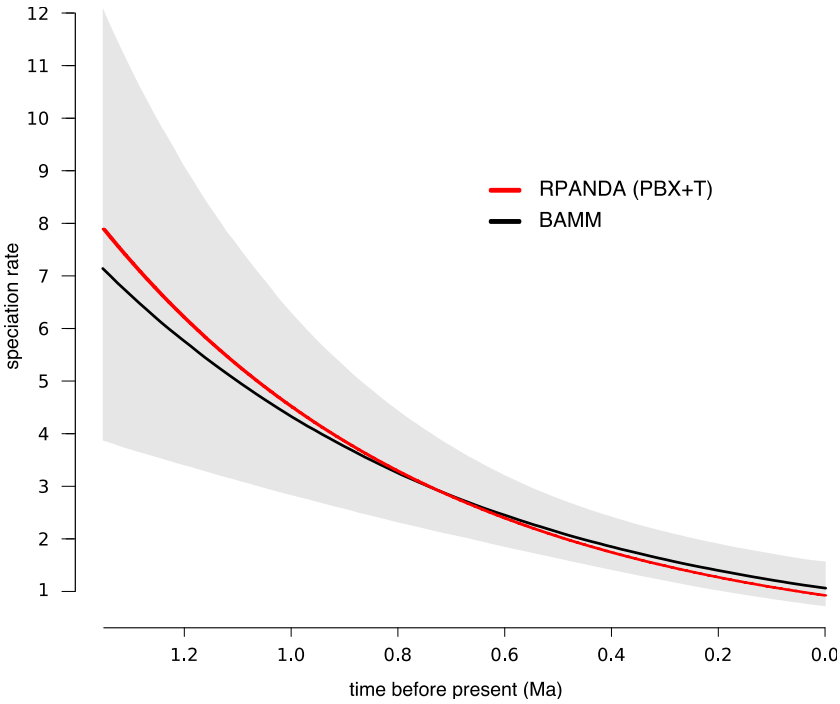


**Literature cited:**

Rabosky, D.L., Grundler, M., Anderson, C., Title, P., Shi, J.J., Brown, J.W., *et al*. (2014). BAMMtools: an R package for the analysis of evolutionary dynamics on phylogenetic trees. *Methods in Ecology and Evolution*, 5, 701–707.

Morlon, H., E. Lewitus, F. L. Condamine, M. Manceau, J. Clavel, and J. Drury. 2016. RPANDA: an R package for macroevolutionary analyses on phylogenetic trees. *Methods in Ecology and Evolution* 7: 589–597.

**APPENDIX S8a.** Contribution of habitat (HAB) and climatic (CLIM) variables into the environmental space, and of vegetative (VEG) and reproductive (REP) trait into the morphological space.

Note: components are represented by black (PC1), grey (PC2) and white (PC3) colors. Analyses were performed with the R package 'ade4' (Dray and Dufour, 2007). Abbreviations for traits are given in the Table 1.

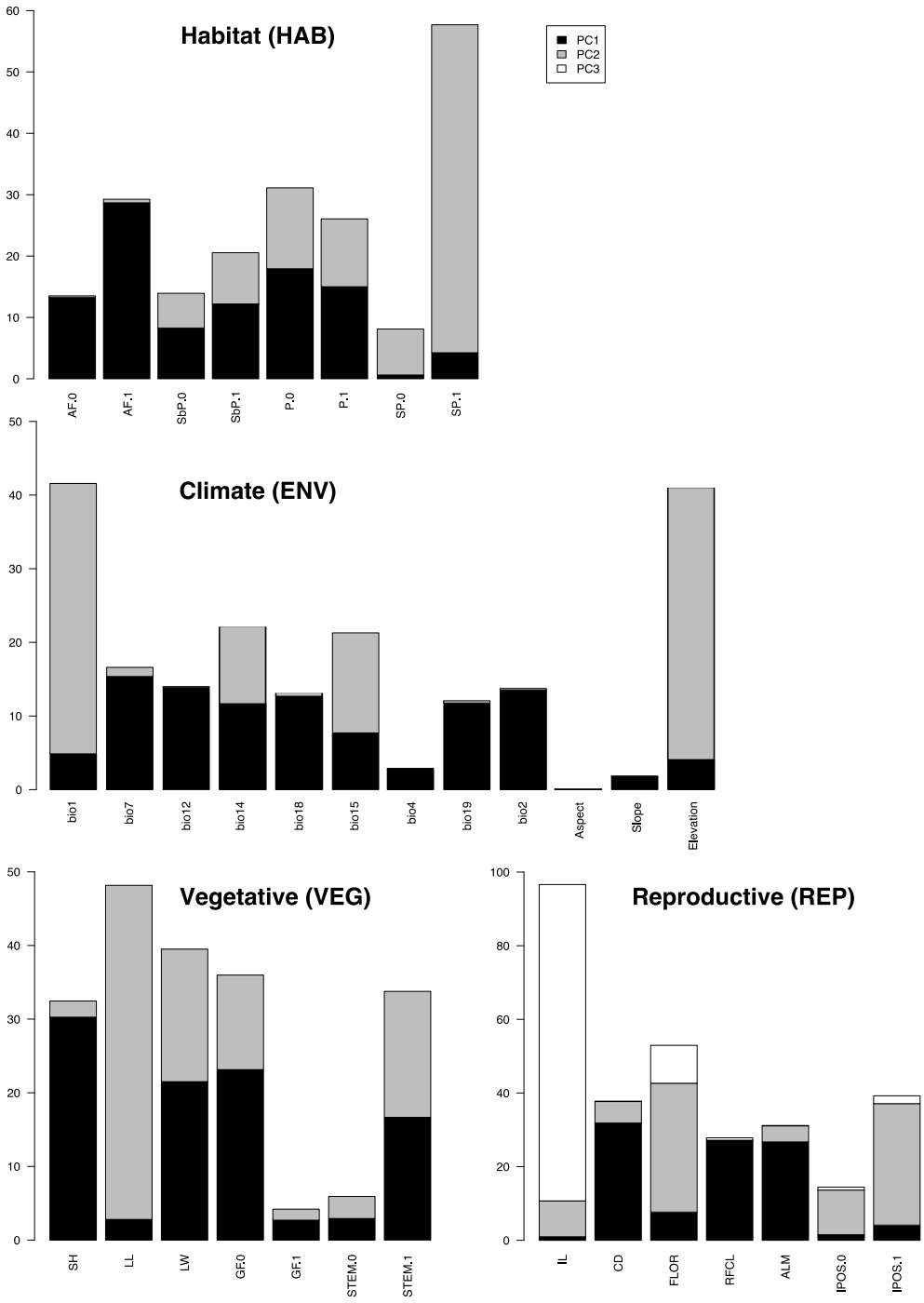

**APPENDIX S8b.** Distribution of species into the first two axes of the (a.) environmental and (b.) morphological space. Environmental component is estimated by the occupied climatic niche space (a.1 – OMI) and the habitat (a.2 – HAB) whereas morphological component is estimated by the occupied vegetative space (b.1 – VEG) and the reproductive space (b.2 – REP).

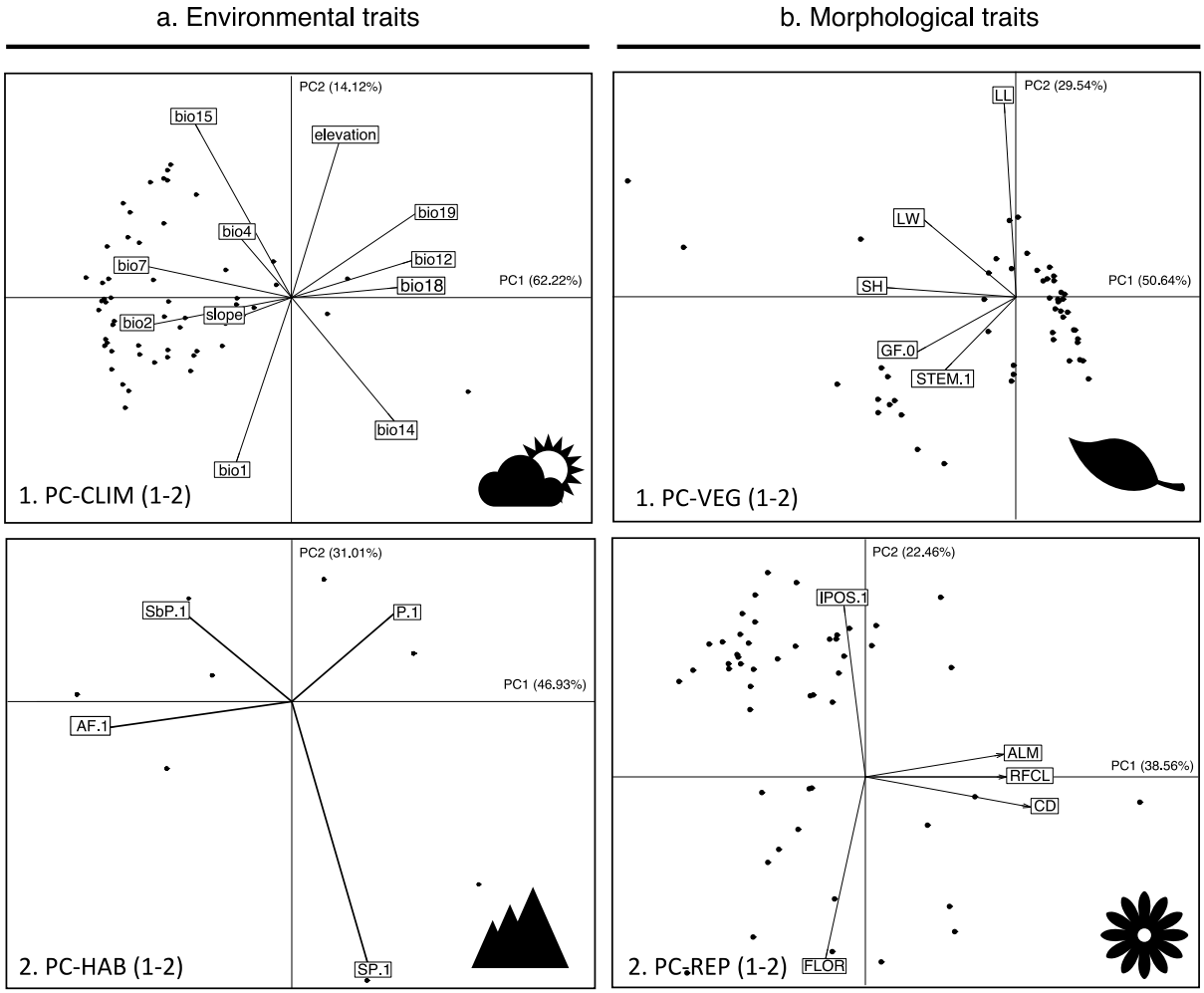

**APPENDIX S8c.** Projection of reproductive space occupied by species for the first (PC1-REP) and the third component (PC3-REP).

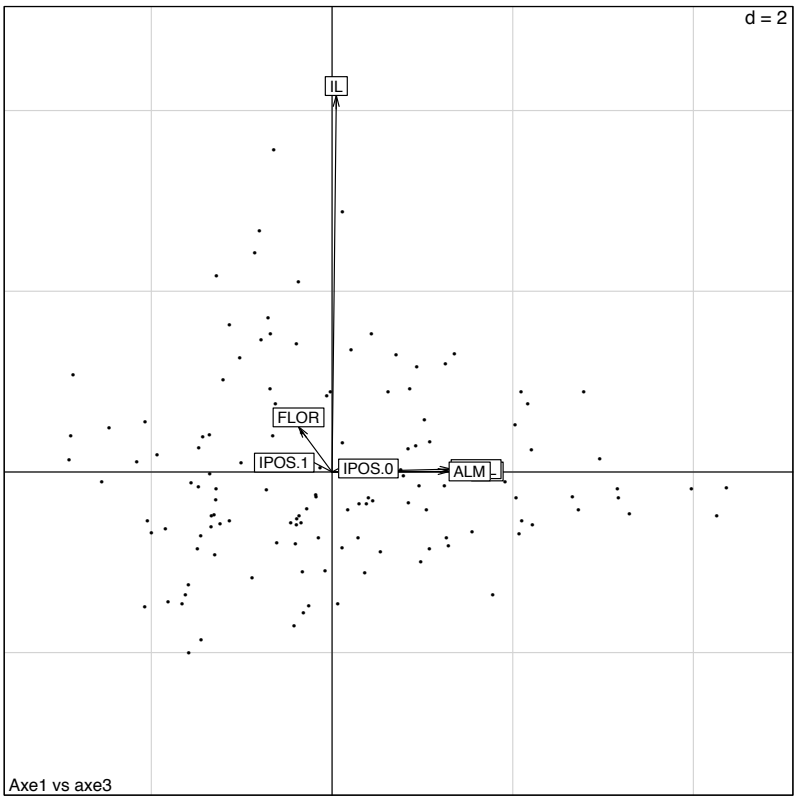

**APPENDIX S8d.** Phylogenetic projection of morphological (PC2-VEG, PC2-REP, PC3-REP) and environmental (PC1-CLIM) space occupied by species.

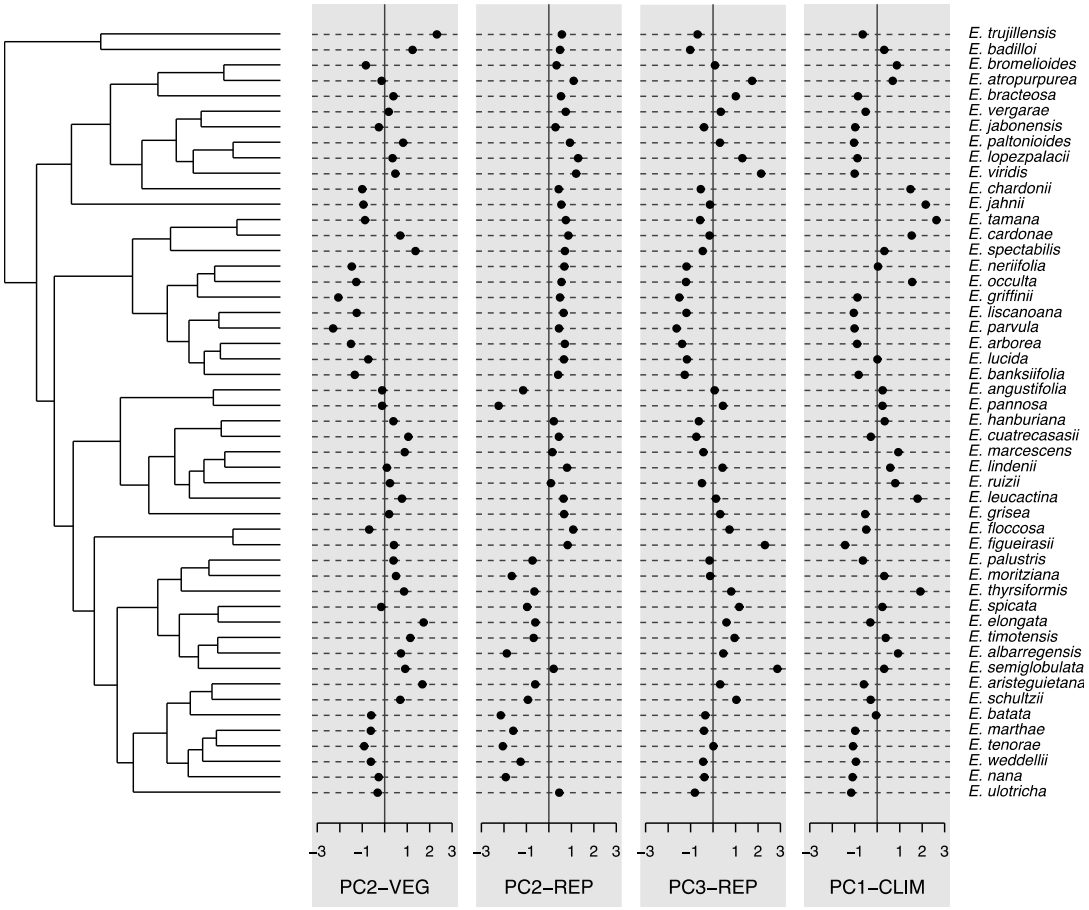


**Literature cited:**

Dray, S. & Dufour, A.-B. (2007). The ade4 Package: Implementing the Duality Diagram for Ecologists. *Journal of Statistical Software*, 022.

**APPENDIX S9a.** Phylogenetic generalized least-squares (PGLS) models assessing the relationship between the Environmental and the morphological space position occupied by species. Pvalues of the likelihood-ratio test were adjusted by Benjamini & Hochberg (1995) method. Regressions were estimated with R packages 'caper' (Orme *et al*. 2018) and 'ape' (Paradis et al., 2004). Note: VEG-Vegetative component; REP-reproductive component; CLIM-Climatic component; HAB-habitat component.

| | | | Environmental | | | |
|---|---|---|---|---|---|---|
| | | | CLIM | | HAB | |
| Morphological | | | PC1 | PC2 | PC1 | PC2 |
| VEG | PC1 | coefficient | -0.3974 | 0.33135 | 1.21162 | 0.65758 |
| | | likelihood ratio | 1.3167 | 1.8446 | 16.774 | 2.6382 |
| | | adjusted pvalue | 0.456727 | 0.34882 | **0.00085*** | 0.334285 |
| | PC2 | coefficient | -0.14236 | -0.44245 | -0.21208 | 0.47362 |
| | | likelihood ratio | 0.265 | 5.4207 | 0.61281 | 1.938 |
| | | adjusted pvalue | 0.808933 | 0.0995 | 0.667230 | 0.348823 |
| REP | PC1 | coefficient | -0.28247 | 0.58784 | 0.25071 | -0.70283 |
| | | likelihood ratio | 1.9896 | 9.3679 | 1.1616 | 7.6013 |
| | | adjusted pvalue | 0.348823 | **0.02208*** | 0.468540 | **0.03888*** |
| | PC2 | coefficient | -0.10969 | -0.22670 | -0.02534 | 0.039172 |
| | | likelihood ratio | 0.3067 | 2.8064 | 0.019242 | 0.028181 |
| | | adjusted pvalue | 0.808933 | 0.334285 | 0.905 | 0.905 |
| | PC3 | coefficient | -0.02731 | 0.264192 | 0.064983 | 0.13482 |
| | | likelihood ratio | 0.014253 | 2.4576 | 0.068876 | 0.20618 |
| | | adjusted pvalue | 0.904970 | 0.334285 | 0.904970 | 0.81225 |

**APPENDIX S9b.** Phylogenetic generalized least-squares (PGLS) models assessing the relationship between the Environmental space position occupied by species and quantitative traits composing the vegetative (PC1-VEG) and the reproductive (PC1-REP) components. Pvalues of the likelihood-ratio test were adjusted by Benjamini & Hochberg (1995) method. Regression were estimated with R packages 'caper' (Orme *et al*. 2018) and 'ape' (Paradis et al., 2004). Note: ALM-Achene Length Mean; CD-Capitulum Diameter; CLIM-Climatic component; HAB-habitats; LW-Leaf Width; RFCL-Ray Flower Corolla Length; SH-Stem Height.

| | | | Environmental | | | |
|---|---|---|---|---|---|---|
| | | | CLIM | | HAB | |
| Morphological | | | PC1 | PC2 | PC1 | PC2 |
| VEG | SH | coefficient | 16.583 | -74.246 | -316.646 | -207.75 |
| | | likelihood ratio | 0.040747 | 1.606 | 20.587 | 4.6377 |
| | | adjusted pvalue | 0.950916 | 0.37283 | **0.00011*** ** | 0.089364 |
| | LW | coefficient | -0.062642 | -1.54464 | -1.8054 | 0.065164 |
| | | likelihood ratio | 0.00484 | 6.5707 | 4.9839 | 0.00378 |
| | | adjusted pvalue | 0.950916 | 0.05183 | 0.085279 | 0.950916 |
| REP | CD | coefficient | -1.2645 | 4.9041 | 1.5980 | -6.3556 |
| | | likelihood ratio | 0.48268 | 12.682 | 0.9122 | 6.8975 |
| | | adjusted pvalue | 0.649614 | **0.00369**** | 0.48503 | 0.05183 |
| | RFCL | coefficient | -1.36044 | 0.38614 | 1.26453 | 0.10902 |
| | | likelihood ratio | 2.3503 | 0.32353 | 1.617 | 0.008812 |
| | | adjusted pvalue | 0.278351 | 0.71186 | 0.372832 | 0.950916 |
| | ALM | coefficient | -0.10651 | 0.103881 | -0.184016 | -0.28095 |
| | | likelihood ratio | 1.1392 | 1.3224 | 3.378 | 5.3889 |
| | | adjusted pvalue | 0.439724 | 0.416934 | 0.165176 | 0.08106 |

**Literature cited:**

Benjamini, Y. & Hochberg, Y. (1995). Controlling the False Discovery Rate: A Practical and Powerful Approach to Multiple Testing. *Journal of the Royal Statistical Society*. *Series B (Methodological)*, 57, 289–300.

Orme, D., Freckleton, R., Thomas, G., Petzoldt, T., Fritz, S., Isaac, N., *et al*. (2018). *caper: Comparative Analyses of Phylogenetics and Evolution in R*.

Paradis, E., cre, cph, Blomberg, S., Bolker, B., Brown, J., *et al*. (2019). *ape: Analyses of Phylogenetics and Evolution*.

**APPENDIX S10a.** Fitted models of trait evolution explored for PC1-VEG and PC1-REP morphological components. Models analysed were BM-Brownian Motion model; OU- Ornstein-Uhlenbeck; EB-Early Burst model; DDL-Linear diversity-dependent model; DDX-Exponential diversity-dependent model; MC-Matching Competition model. Note: AICc- corrected Akaike Information Criterion, Loglik: log-likelihood. Models BM, OU and EB were fitted in the R package 'geiger' (Harmo*n et al*., 2008) whereas models MC, DDL and DDX were fitted in 'RPANDA' (Morlon et al., 2016).

| | PC1-VEG | | | PC1-REP | | |
|---|---|---|---|---|---|---|
| Model | Loglik | AICc | Parameters | Loglik | AICc | Parameters |
| White | -112.99 | 230.244 | sigsq= 5.375<br>z0=-0.493 | -71.328 | 146.913 | sigsq=1.015<br>z0=-0.662 |
| BM | -92.019 | 188.293 | sigsq= 3.412<br>z0=-2.480 | -68.683 | 141.623 | sigsq=1.341<br>z0=-1.020 |
| OU | -92.019 | 190.560 | α=0.000; sigsq= 3.412; z0= -2.480 | -66.999 | 140.521 | α=1.050; sigsq= 2.333; z0=-0.873 |
| EB | -89.354 | 185.230 | a=-1.434; sigsq= 12.720; z0=-3.072 | -68.683 | 143.889 | a=-1e-6; sigsq = 1.341; z0=-1.020 |
| DDL | -90.509 | 187.541 | b=-0.067; sigsq= 5.857; z0=-2.713 | -66.896 | 140.315 | b= 0.032; sigsq= 0.116; z0=-0.874 |
| DDX | -90.025 | 186.573 | r=-0.024; sigsq= 7.604; z0=-2.813 | -66.850 | 140.222 | r= 0.037; sigsq= 0.284; z0=-0.906 |
| MC | -88.53 | 183.587 | S=-0.825; sigsq= 1.731; z0= -1.841 | -68.683 | 143.889 | S=-3e-8; sigsq= 1.341; z0= -1.020 |
| Delta | -86.94 | 180.403 | d= 0.1745; sigsq= 11.325; z0= -4.039 | -67.027 | 140.577 | d= 2.543; sigsq= 0.781; z0= -0.837 |

**APPENDIX S10b.** Fitted models of trait evolution explored two traits independently correlating to environment: stem height (SH) and the capitulum diameter (CD). Estimations were done for the consensus-dating tree. Models analysed were BM-Brownian Motion model; OU- Ornstein-Uhlenbeck; EB-Early Burst model; Delta model; DDL-Linear diversity-dependent model; DDX-Exponential diversity-dependent model; MC-Matching Competition model. Note: AICc- corrected Akaike Information Criterion, Loglik: log-likelihood. Models BM, OU, Delta and EB were fitted in the R package 'geiger' (Harmo*n et al*., 2008) whereas models MC, DDL and DDX were fitted in 'RPANDA' (Morlon et al., 2016).

| | SH | | | CD | | |
|---|---|---|---|---|---|---|
| Model | Loglik | AICc | Parameters | Loglik | AICc | Parameters |
| White | -88.683 | 181.623 | sigsq= 2.032<br>z0= 0.194 | -69.037 | 142.330 | sigsq= 0.926<br>z0= -0.301 |
| BM | -77.258 | 158.772 | sigsq= 1.890<br>z0= 1.453 | -58.584 | 121.423 | sigsq= 0.895<br>z0= -0.695 |
| OU | -77.258 | 161.038 | α=0.000; sigsq= 1.890; z0= 1.453 | -58.221 | 122.964 | α= 0.429; sigsq= 1.156; z0=- 0.631 |
| EB | -76.475 | 159.473 | a=-0.866; sigsq= 4.353; z0= 1.698 | -58.584 | 123.689 | a=-1e-6; sigsq = 0.895; z0= -0.695 |
| DDL | -76.990 | 160.502 | b=-0.017; sigsq= 2.526; z0=1.533 | -58.143 | 122.808 | b= 0.013; sigsq= 0.405; z0=-0.635 |
| DDX | -76.902 | 160.327 | r= -0.011; sigsq= 2.832; z0= 1.563 | -58.210 | 122.94 | r= 0.015; sigsq= 0.490; z0=-0.650 |
| MC | -75.955 | 158.433 | S=- 0.558; sigsq= 1.254; z0= -1.184 | -58.584 | 123.689 | S=-2e-6; sigsq= 0.895; z0= -0.695 |
| Delta | -74.727 | 155.976 | d= 0.282; sigsq= 4.539; z0= 2.334 | -58.069 | 122.661 | d= 1.684; sigsq= 0.650; z0= -0.586 |

**Literature cited:**

Harmon, L.J., Weir, J.T., Brock, C.D., Glor, R.E. & Challenger, W. (2008). GEIGER: investigating evolutionary radiations. *Bioinformatics*, 24, 129–131.

Morlon, H., Lewitus, E., Condamine, F.L., Manceau, M., Clavel, J. & Drury, J. (2016). RPANDA: an R package for macroevolutionary analyses on phylogenetic trees. *Methods in Ecology and Evolution*, 7, 589–597.

**APPENDIX S11.** Assembly of *Espeletia* communities in the páramo of Piedras Blancas (Venezuela) according to ecological preferences of species according to moisture and slope.

Topographic and vegetation sequence for the Espeletiinae distribution for sympatric and closely related species according to moist sol and slope gradient. Profile was made according to Pérez (1996) and field observations in the páramo Piedras Blancas. Phylogeny represents clade VII (here 1) and VIII (here 2) estimated in Chapter 2. Only sympatric species of these clades are shown in the profile and in the phylogenetic tree by solid branches. Acronyms represent species names with: AL-*Espeletia albarregensis*, BA-*E. batata*, EL-*E. elongata*, MA-*E. marthae*, MO-*E. moritziana*, PA-*E. palustris*, SC-*E. schultzii*, SE-*E. semiglobulata*, SP-*E. spicata*, TE-*E. tenorae* and TI-*E. timotensis*.

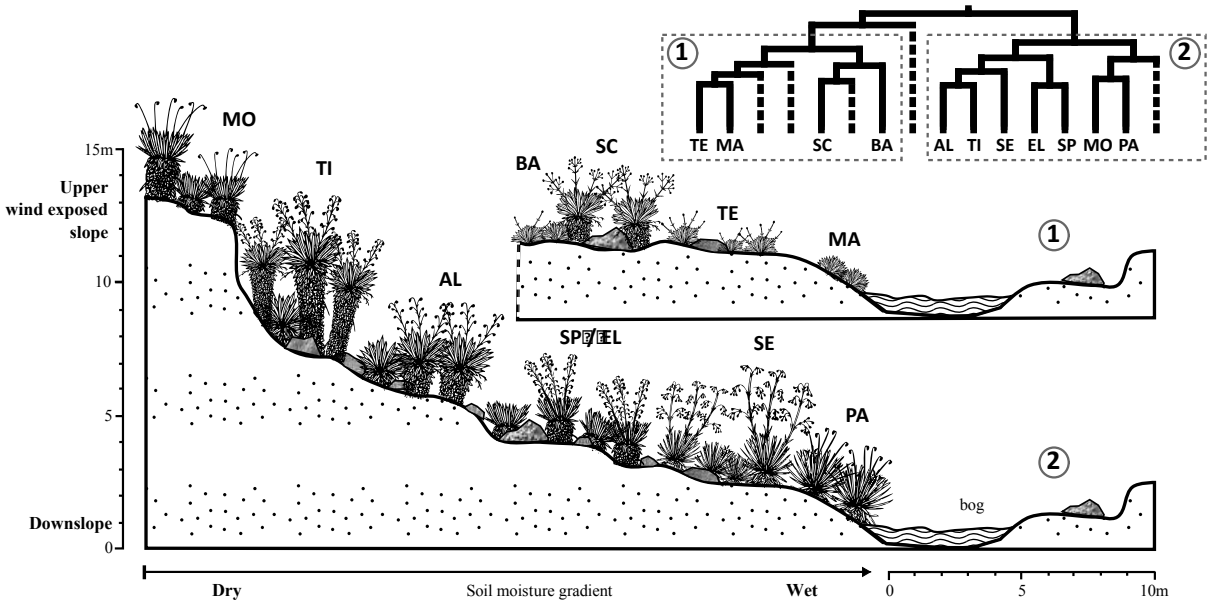


**Literature cited:**

Pérez, F.L. (1996). The effects of giant Andean rosettes on surface soils along a high paramo toposequence. *GeoJournal*, 40, 283–298.